修士論文

Walking Motion Control of Biped Robotic Legs Inspired by Human Muscle Model for Adapting Variation of Vertical Load

鉛直方向の負荷変動に対応する２足歩行の運動制御 ―生体の筋構造の考慮の有無による相違の評価

2012年2月8日

指導教員
古関隆章 准教授
東京大学大学院工学系研究科
電気系工学専攻 No. 37-106907

Emre DUMAN

Abstract

Research on biologically inspired robots is advancing nowadays. Researhers observe mechanical properties and dynamic motions of many biological objects and such observations are used in order to implement on some robotic systems which can have similar characteristics. Many industrial robots and humanoid robots such as ASIMO, AIBO, QRIO are conventional type robots. Conventional humanoid robots and biological subjects differ in their mechanisms and control strategy. Biological subjects have musculoskeletal systems that can drive two joints at the same time while conventional robots use one joint drive mechanisms. Biological objects use their monoarticular and biarticular muscles in order to move their limbs and they have nearly perfect coordination of those muscles while jumping, landing, biped walking, running, etc. Muscle mechanism makes it easier to exert more force at the tip and the distribution of forces can be varied based on each activation of muscles. In this research, a biped robotic leg which is inspired by human leg muscle model is taken into account and walking behaviour of the leg in the existance of an external force is analised. Details of the mathematical modeling for such biologically inspired robotic leg is explained and simulation results for joint torque generation for different situations, especially in case of an vertical external force are presented. It has been shown that human has rational mechanism for output force control at the tip by taking the advantage of cooperative actuation of monoarticular and biarticular muscles. Especially, the magnitude of force is bigger in the direction from the fixed joint to the end effector. Human use this advantage for carrying a heavy body and also for jumping, walking and rejection of external forces. Additionally, using biarticular muscle improves the self-stability of the robotic leg by transfering energy between two adjacent joints. Dynamic motion is theorotically derived by taking mass, inertia, link lengths and gravity into account. Walking for robotic leg is formulated for both legs, one is when leg is carrying the body and react to external force, other is when leg is not in contact with the ground and taking one step forward. Joint torques are distributed to individual muscles by using a method called 2-norm which is used to calculate the efficient way of distribution of 2 values into 3. As for muscle model, a spring-damper system is considered so that flexibility can be achieved and, DC motor is used as actuator to tighten and loosen the muscle. Wires are used in order to transfer rotational motion into translational motion. Each muscle is controlled by a DC motor after calculating the necessary displacements of each muscles.

Acknowledgement

First of all, I would like to give my gratitudes to my two advisors; Prof. Koseki Takafumi and Prof. Hashimoto Hideki for giving me a chance to study in their laboratories and for their supports in my research. They gave me the opportunity and freedom to study on what interests me the most, so that i could had a chance to study on something i enjoy. Special thanks to Prof. Koseki Takafumi who always supported and encouraged me to advance in this work by giving very precious advices and comments, and also trying to answer all of my questions kindly.

I thank all the Professors at Department of Electrical Engineering and Information Systems in The University of Tokyo for helping me to expand my knowledge in all the latest technologies and for giving valuable feedback in “Rinkou” presentations.

I thank all my past and present colleagues at Hashimoto Laboratory and Koseki Laboratory for providing a warm and friendly working environment, i will never forget the friendships i have gained in the period of my stay in Japan.

I am grateful for all my Turkish friends residing in Japan, who made life in Japan easier, for being a welcome distraction from university life, listening my problems and trying to support me.

I thank my wonderful wife, Kyoko, for her unconditional love and continuous support regardless of the situations, especially for encouraging me at frustrating times and taking care of me when i got sick.

Finally, I would like to express my sincere gratitude towards my parents; my father and mother for their understandings and encouragement of pursuing my graduate study in Japan, and my siblings for their psychological support.

Table of Contents

List of Tables

List of Figures

Chapter 1

Introduction

In this chapter, after giving a brief introduction, some of current researches related to humanoid robots will be presented and the motivation of the this research will be explained. Finally, an organization chart of thesis will be provided.

1.1 Research Background

Technologies related to humanoid robots are advancing in the last years. Some researchers concentrate on control of robotic arms and some concentrate on control of robotic legs. ASIMO from HONDA, QRIO from Sony, and KONDO VHR series walking robots can be given as examples of the most well-known walking robots. The similarity between these robots is that all of them are controlled with the actuators placed on their joints, which is generally called conventional type. Besides these models, emulation of life mechanisms has also attracted many researchers' attentions since the late years of 20^{th} century. In order to develop biologically inspired robot manipulators, observation of human and animal characteristics are essential. Some researchers are focusing on to gather living mechanism's dynamic gaits like [1][2] while others try to use those features to apply on their robotic systems like [3][4]. By analyzing the musculoskeletal systems of human and animals, robot arms[6][10] and legs[5][7][8] that mimic their behaviors, are modeled and controlled. Moreover, some power assisted devices are also designed to support elderly and disabled people or to increase the performance of workers or soldiers who perform difficult tasks and are carrying heavy loads.

1.2 Current Researches related to Biologically Inspired Robots

ASIMO(Figure 1.1.a) is created by HONDA in 2000, its weight is about 48 kg and height is 130 cm. It is created to perform walking, running and climbing the steps as well as interacting with humans. Robot can detect moving objects, sounds and faces. It has a walking speed of 2.7 km/h and a running speed of 9 km/h. Its balance is achieved by reaction force control and ZMP(Zero Moment Point) so that it can adjust its posture. Its knees have one degree of freedom, ankles have two degrees of freedom and hips have three degrees of freedom.

QRIO(Figure 1.1.b) is created by SONY in 2006, its weight is about 7.3 kg and height is 60 cm. It can perform a dance, recognize voice and face. It can run at 23 cm/s. AIBO(Figure 1.1.c) is also created by SONY in 1999. Robotic pet AIBO is capable of walking and recognizing voice commands.

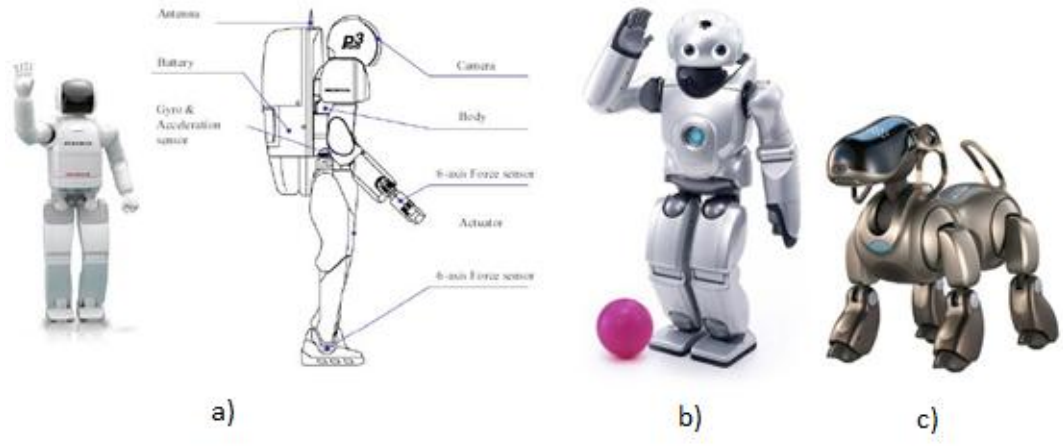

Figure 1.1 Famous walking robots a)ASIMO b)QRIO c)AIBO

BigDog(Figure 1.2) is a quadro-legged robot that is inspired by dog and created by Boston Dynamics. It has hydraulic actuation mechanism with compliant elements to absorb shocks which is very similar to animals. Its weight is 109 kg and height is 76 cm. It is designed with the capability of walking, running, climbing and carrying heavy loads in rough terrains. Its control systems make robot adapt to varying conditions. The goal of that project is to develop a robot that is able to go anywhere animals and humans can.[11]

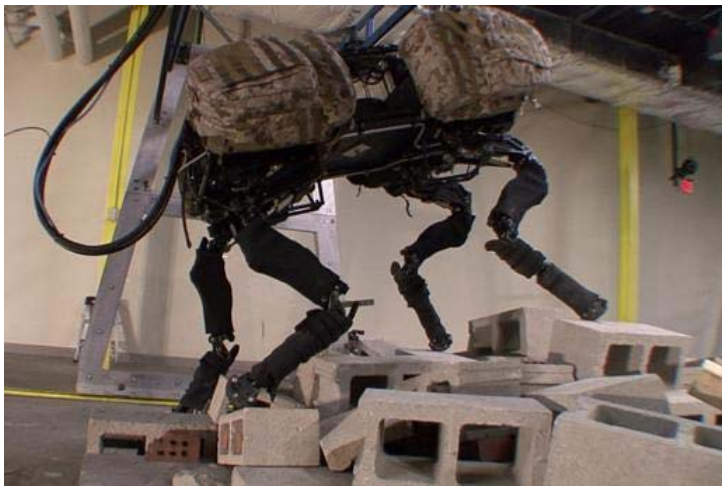

Figure 1.2 BigDog from Boston Dynamics[11]

Other than biologically inspired humanoid and quadro-legged robots, there are also some power assist devices that are designed to help or assist humans who are disabled or working in jobs that requires heavy loads to carry. Some of those devices are shown in Figure 1.3

Rex, the Robotic Exoskeleton (Figure 1.3.a) is designed by Rex Bionics. It is a pair of legs which enables wheelchair users to stand, walk and step up or down, allowing them to be more mobile. It also has a joystick control to direct the device for sitting and turning. Moreover, it also has self supporting ability that enables users to use their arms and hands freely.

HAL is a robotic suit designed by Cyberdyne. It has a variety of uses where power assisting is needed, especially for disabled and elderly people, people who are working in physically demanding jobs and in rescue support in disaster sites. This suit can read nerve signals and tries to move the robotic suit according to reading. This suit enables user to lift and carry five times more weight compared to her or his capability without using the suit.

Figure 1.3 Power Assist Devices a) Rex b) HAL

1.3 Motivation

As the technology related to robotic systems are advancing, realization of using characteristic properties of living things effects the thoughts of some researchers. They also try to advance the technology related to human-robot interaction and natural response to environmental changes around robots. In this research an application of mimicking a human leg is considered. The main objective is the modeling of such biologically inspired robotic leg with combined monoarticular and biarticular muscles and achieving successful walking control in the existence of external forces acting on the body in simulation environment. It is expected to achieve safer and more human-like motion of a robotic leg against external forces by using muscle model. Using monoarticular and biarticular muscles can improve the maximum external force rejection capability. It will be tried achieve low trajectory error as in conventional method; but it seems difficult to have perfect trajectory tracking because of the distributed control of muscles and the elasticity of muscles. Moreover, by using the advantage of biarticular muscle in

self-stability of the robotic leg, it is expected to improve the self-stability of the leg.

1.4 Organization Chart

- In Chapter2, the role of monoarticular and biarticular muscles will be explained and muscles of human leg will be given as examples. After giving some information of some researches related to monoarticular and biarticular muscles, the advantages and disadvantages of using them will be discussed. Moreover, the distribution of the end effector force will be explained in the case of using biarticular muscle, and compared with the conventional type.

- In Chapter 3, theoretical and mathematical representations of robotic leg with muscle model will be provided in detail. After giving the outline of the robotic leg motion, walking scheme, trajectory planning, calculations for angles, angular velocities, angular accelerations and joint torques will be presented. The method to calculate individual muscle torques from joint torques will be explained. Moreover, the effect of external forces on joint torques will be given and the strategy to reject that force will be explained. Resulted muscle displacement calculations will be shown and the method to control each muscle torque will be discussed. Finally, control diagram for muscles will be provided.

- In Chapter4, parameters that are used in the simulation will be given. Then, simulation results for different external forces in conventional model and muscle model will be shown in terms of position tracking performance and maximum external force rejection capabilities. Moreover, simulations will be done in two different cases to show the efficiency of using biarticular muscles. Discussion and comments about simulation results will be given and the comparison between various methods will be discussed.

- In Chapter5, summary and conclusions related to this research will be given. Then, this paper will be concluded by presenting some of future works.

Chapter 2

The Role of Monoarticular and Biarticular Muscles on Joint Torques and End Point Force

In this chapter, the role of monoarticular and biarticular muscles will be explained and muscles of human leg will be given as example. After introducing some researches related to monoarticular and biarticular muscles, the advantages and disadvantages of using them will be discussed. Moreover, the distribution of the end effector force will be explained in the case of using biarticular muscle, and compared with the conventional type.

2.1 Outline of Muscles in Human Leg

Human and animals use various types of muscles for hopping, walking, jumping, running and other dynamic actions. Joint torques on their knees, ankles and hips are generated with the coordination of different muscles. An example of muscles in human leg is shown in the Figure 2.1 below. Especially, Gastrocnemius muscle is studied by many researchers.

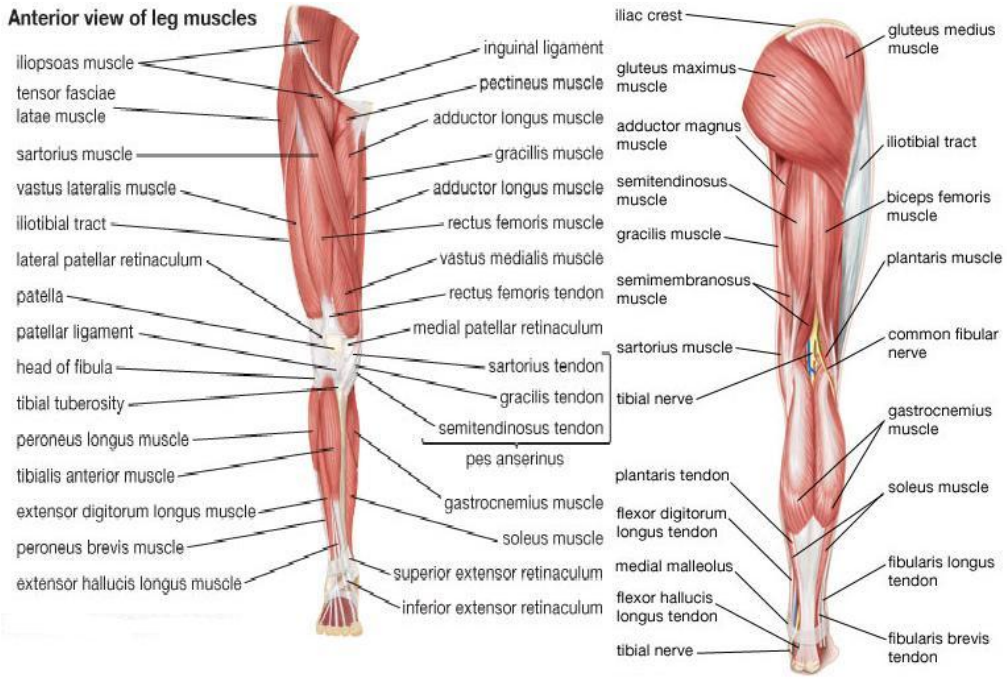

Figure 2.1 Muscles in human leg

Muscles are generally divided into two types, which are flexors (biceps) and extensors (triceps). Working principle of those muscles can be summarized as follows,

- Flexors (Biceps): These muscles are used to flex the links. When they are activated, the angle between links are decreased.

- Extensors (Triceps): These muscles work oppositely to flexors. They are used to extend the links. When they are activated, the angle between links are increased.

Most of researchers tried to make a model of human leg by using artificial muscles and the mostly used model in those researches is as in the Figure 2.2

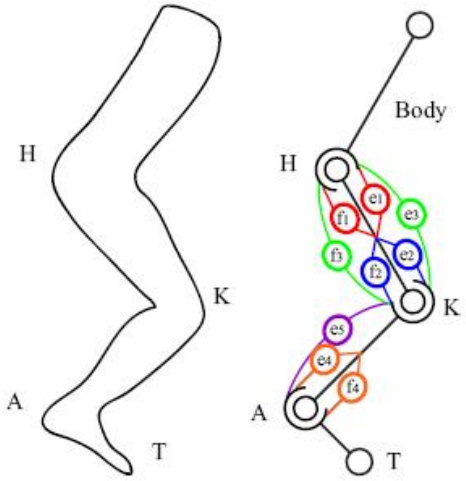

Figure 2.2 The model of human leg

In this model; e1, e2, e3 and e4 denote extensors and f1, f2, f3, f4 denote flexors. The pairs of e1-f1, e2-f2 and e4-f4 generate torques around hip, knee and ankle joints respectively. The couple e3-f3 and the extensor e5 generate torques around both hip and knee joints, and knee and ankle joints respectively.

Such muscles are also categorized in two types, which are monoarticular muscles and biarticular muscles. Properties of these muscles can be summarized as follows,

- Monoarticular muscles: These muscles are connected to a link and a joint. They can drive only one joint by producing torque around that joint.

- Biarticular muscles: These muscles are connected to two adjacent joints and can drive these two joints simultaneously. The magnitudes of the torque that are produced around two joints are the same.

Muscles #1, #2 and #4 are monoarticular muscles, #3 and #5 are biarticular muscles in Figure 2.2

Researchers observe the motion of living things and their muscle characteristics, then try to make use of such muscles in their robotic systems. The current famous robots like ASIMO and QRIO are two examples of conventional methods; but muscle model is different from that model. In the conventional model, the actuators are on the joints and the number of actuators are equal to number of joints. Rotational motors are used in order to drive hip, knee and ankle joints. On the other hand, in muscle model, actuators are not on the joints but between them. The number of actuators are mostly bigger than the number of joints in this method. Generally, artificial muscles with similar characteristics to muscles in living things, linear actuators or DC motor with a wire driven system are used. The basic model of these two method can be represented as in Figure 2.3

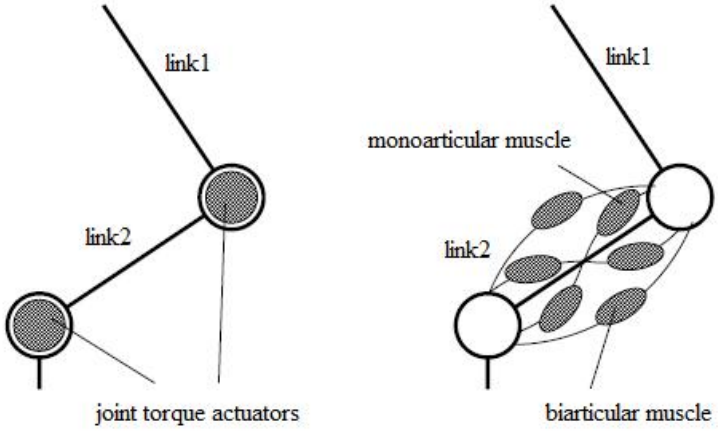

Figure 2.3 Conventional robot model vs muscle model

2.2 Researches related to Mono and Biarticular Muscles

In this part, some of robotic legs that uses monoarticular and biarticular muscle mechanisms will be presented. Since monoarticular and biarticular muscles are advantageous in large instantaneous forces, this mechanism is mostly used in hopping and jumping robots. Usage of artificial musculoskeletal system in walking and running robots are still advancing. One of examples of jumping robots is shown in Figure 2.4

MOWGLI(Figure 2.4) is a pneumatically actuated bipedal robotic leg designed by The University of Tokyo. Six McKibben type pneumatic muscle actuators are used and it has two legs with hip, knee and ankle joints. It is capable of jumping heights of more than 50% of its body height and land softly. Extensions in the whole body motion are caused by the natural characteristics of legs. Experiments are conducted with two types of open loop controllers for vertical jumping with disturbance. In the first experiment robot performs vertical jumping(Figure 2.4.a) and the jumping height between toe and the ground is about 26 cm. Applied control is just turning the valves on and off during the motion. In the second experiment(Figure 2.4.b), robot performs jumping onto a chair of 40 cm height. The same control method is used also in this experiment. The compliance of the leg enables it to land softly to ground. They have demonstrate the contribution of artificial muscle system as a physical feedback loop in explosive motions.[12]

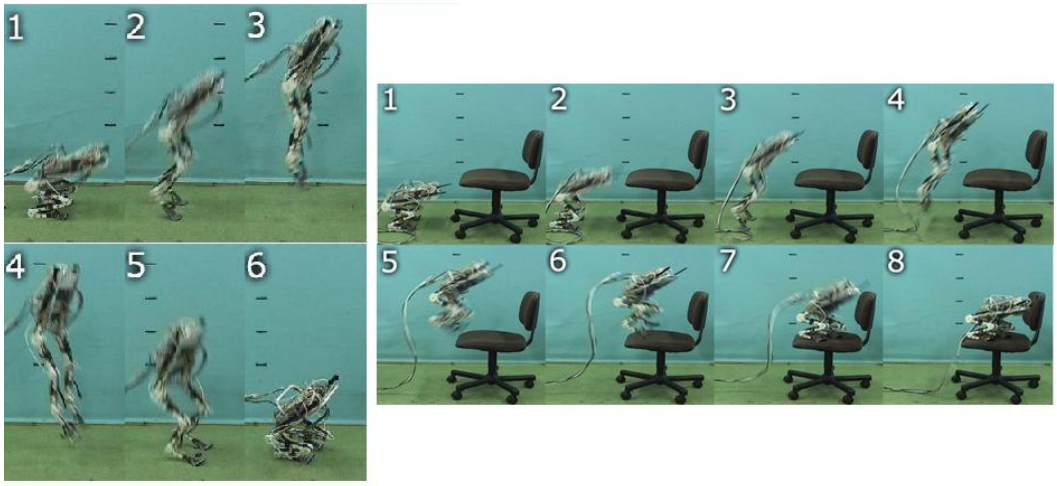

Figure 2.4 MOWGLI: A bipedal jumping and landing robot
a) vertical jumping b) jumping onto chair[12]

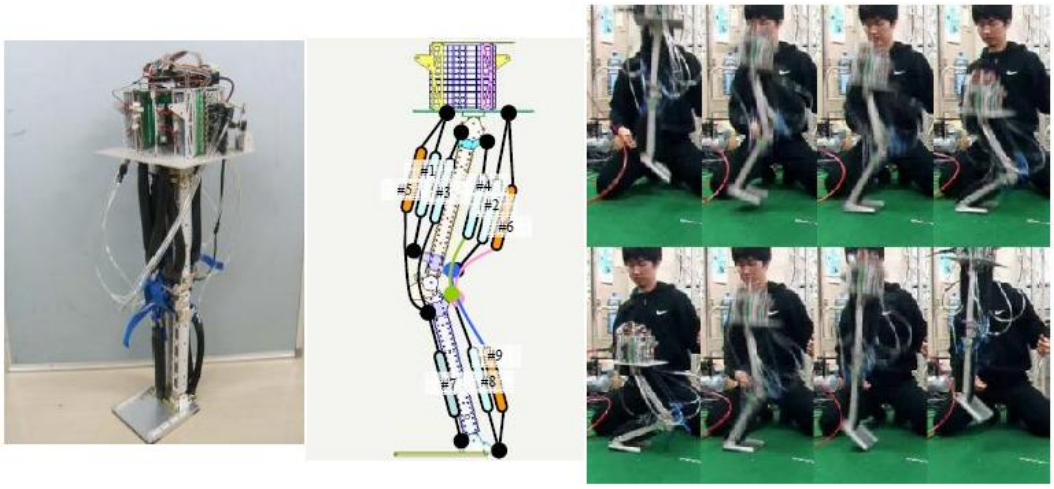

Figure 2.5 Bouncing monopod Kukyaku-K with bio-mimetic muscular-skeleton system[13]

Kukyaku-K (Figure 2.5) is a monopod that uses pneumatic artificial muscles and tries to mimic human leg for dynamic bouncing motion. It has total of 9 actuators, 6 monoarticular and 3 biarticular types. They have confirmed that biarticular muscles govern the coordinated motion of the robot and a simple controller could be able to realize stable bouncing motion although pneumatic actuators have complicated characteristics.[13]

The bipedal robotic leg shown in Figure 2.6 consists of three leg parts with passive knee and ankle joints that are controlled by four linear tension springs. In this research, they have found that the arrangements of the springs which correspond to rectus femoris, biceps femoris and gastrocnemius in human legs help robot to self-stabilize itself for both walking and running gaits. The experimental results also show that a simple oscillation at the actuated hip joints is enough to produce walking and running gaits without feedback if the compliance of leg is properly adjusted.[5]

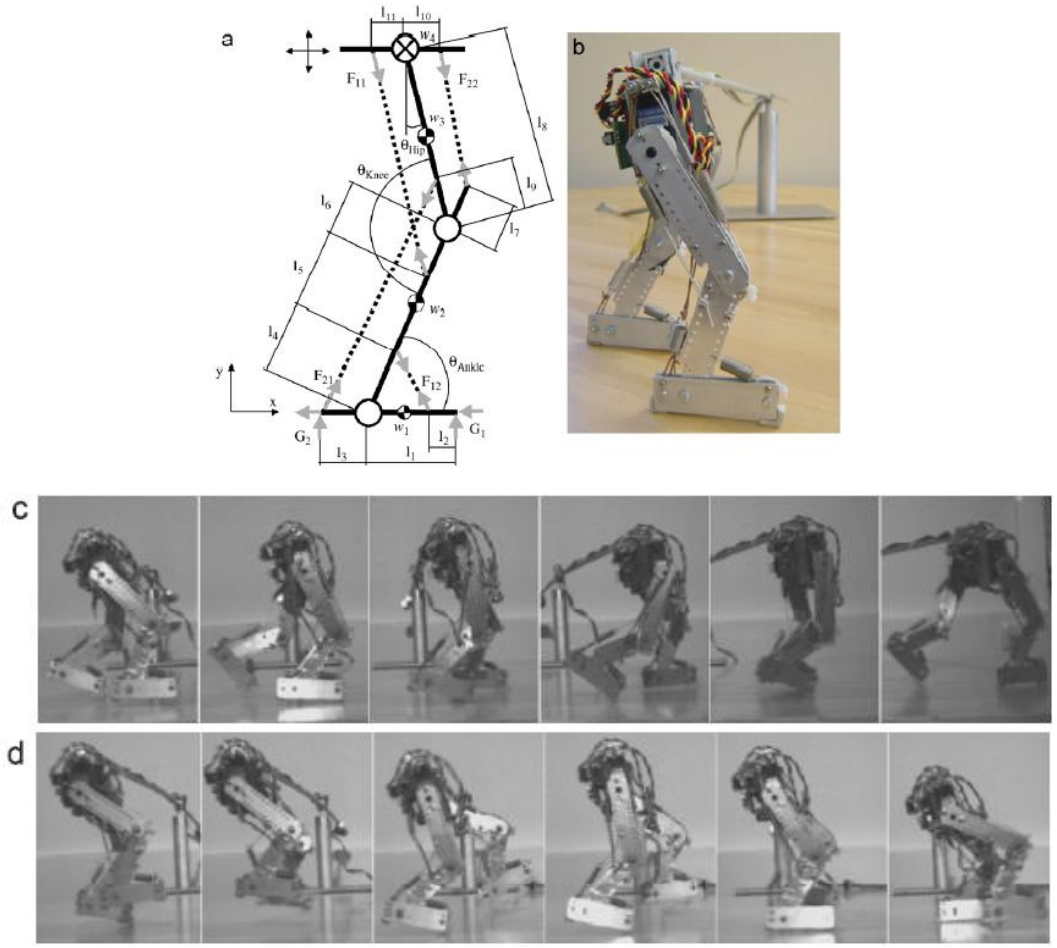

Figure 2.6 Compliant leg model(a)(b) and experiments for walking(c) and running(d)[5]

2.3 Significance and Advantages of using Muscle Model

Advantages of using Biarticular Muscles can be summarized as follows:

- Biarticular muscles transfer mechanical energy from proximal joints to distal joints. It is very useful to use such muscles when motions that high torques are needed. Since the torque is distributed to more actuators, the total torque that can be produced on the joints is also large. Some of researches related to that aspect is legged robots for jumping[7], hopping[13], walking[8] and running[5].

- Increased end effector impedance can be achieved by just using feedforward control in case of using biarticular and monoarticular muscles. Because of the elasticity of muscle itself, reaction to disturbances can be improved without using a sensor. This method also can be used in order to improve the walking capability of bipedal robots[5]

- Maximum output force becomes higher and the distribution of end effector force is more homogenous if biarticular muscle mechanism is used.

In spite of such advantages of using biarticular muscles, there are also some disadvantages such as the actuator redundancy problem and its difficulty to achieve coordinated control.

2.4 Characteristics of End Point Force Distribution with the use of Mono and Biarticular Muscle

Force directions are calculated by using EMG(electromiogram) on static conditions. Amplitudes and directions of the end effector force in conventional model and the proposed method differs as it is seen on the Figure 2.7[6] The black parallelogram shows the force directions in conventional model while the hexagonal shape D1～D6 shows the directions in the proposed method. For instance, activation of the muscle f3 will result in a force towards to D3, and activation of e3 will result a force in opposite direction. That is to say, the pairs e3-f3 works oppositely. It is also possible to achieve stiffness control by adjusting the individual muscle forces e3 and f3 without changing the difference between them to keep the joint torque same.

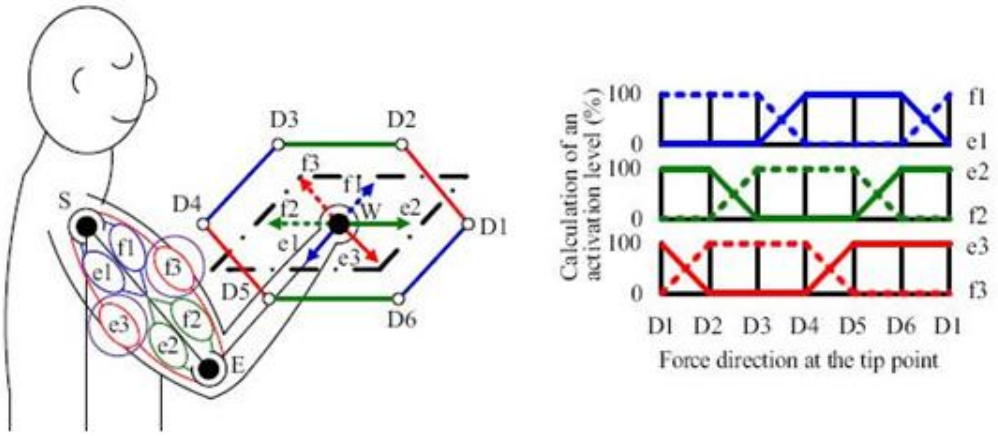

Figure 2.7 Graph of force direction according to each muscle activation

The same principle is also valid for robotic leg with monoarticular and biarticular muscle mechanism, the resulted graph of end point force distribution according to the posture of the robotic leg is seen in Figure 2.8

From this figure, it can be said that the magnitude of the force becomes bigger in the direction from hip to ankle as knee angle degrees and robotic leg stretches. Since knee angle is expected to be small in walking motion of the robotic leg, this advantage is thought to be useful especially in walking with high load and the reaction to external force in vertical direction.

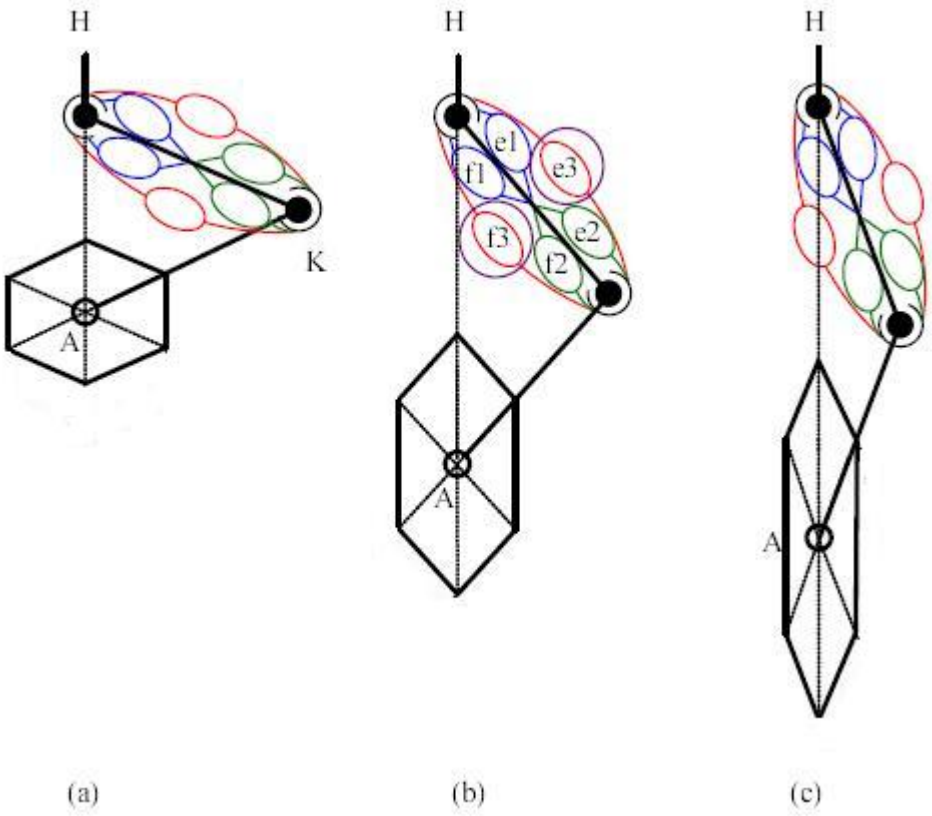

Figure 2.8 End effector force diagram for different postures

2.5 Summary of Chapter

After giving a brief review of previous and on-going researches, the advantages and disadvantages of using monoarticular and biarticular muscles for simultaneous drive of two joints is explained. Then, the difference between conventional robot control method and proposed method is clarified. Moreover, the distribution of the end effector force is explained in the case of using biarticular muscle, and compared with the conventional type.

Chapter 3

Theoretical and Mathematical Representation of Robotic Leg with Muscle Model

In this chapter, after mathematical explanation of the robotic leg that is used in this research is provided, calculations for angles, angular velocities, angular accelerations and torques will be shown in detail. Moreover, in the existence of external forces, the effects of those forces on the joint torques and individual muscle torques will be presented. Furthermore, the details of the muscle model and how to control the muscles will be explained.

The notations used in this section is given in Table 3.1. The general scheme of calculations are shown in Figure 3.1

Table 3.1 Table of parameters

Parameters	Explanation	Units
T_1, T_2, T_4	Monoarticular muscle torques	Nm
T_3, T_5	Biarticular muscle torques	Nm
τ_1	Hip joint torque	Nm
τ_2	Knee joint torque	Nm
τ_3	Ankle joint torque	Nm
m_1, m_2	Mass of links	kg
ℓ_1, ℓ_2	Length of links	m
ℓ_{c1}, ℓ_{c2}	Center of masses of links	m
r	Radius of links	m
I_1, I_2	Inertia of links	$kg.m^2$
g	gravity	m/s^2
r_j	Radius of Joints	m
θ_1	Hip Joint Angle	rad
θ_2	Knee Joint Angle	rad
θ_3	Ankle Joint Angle	rad
F	External Force	N
q	position	m
t	time	s

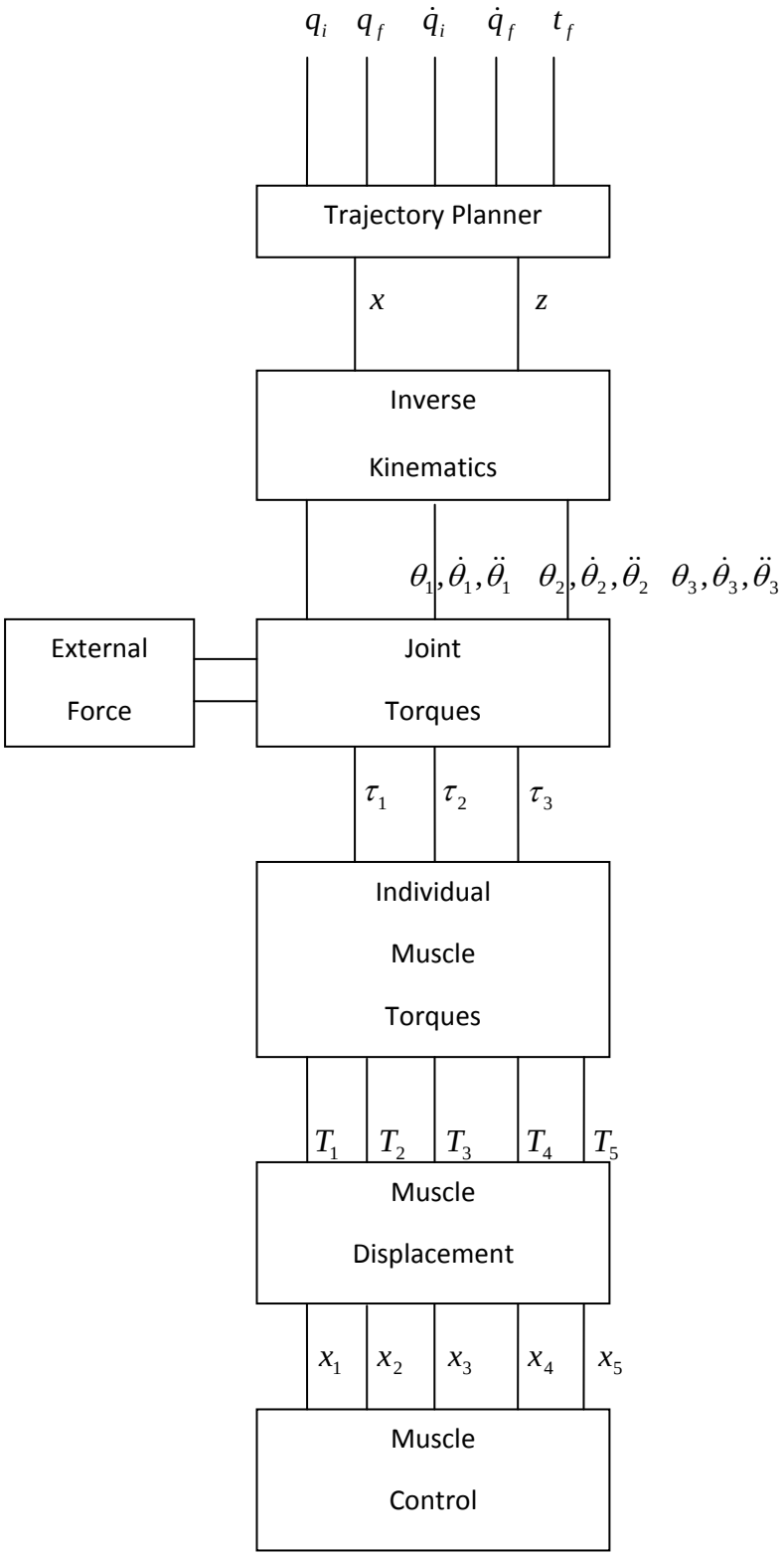

Figure 3.1 General scheme of calculations

3.1 Outline of the Robotic Leg Model with Mono and Biarticular Muscle

The robotic leg model that is used in the mathematical representation is shown in Figure 3.2

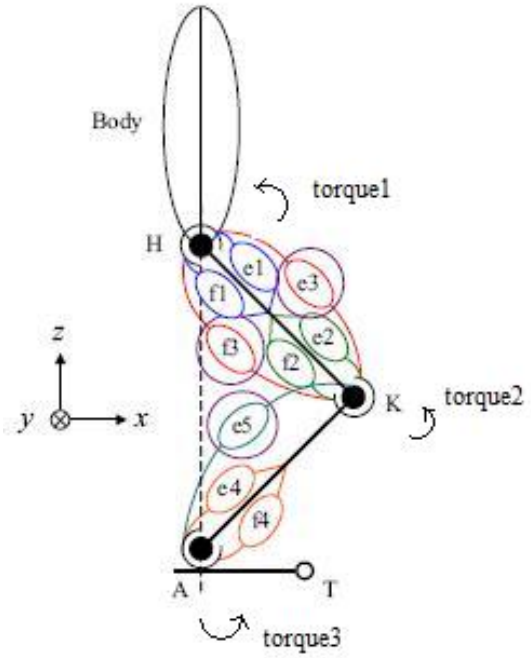

Figure 3.2 Robotic leg model with monoarticular and biarticular muscles

In this model, e1, f1, e2, f2, e4 and f4 represents monoarticular muscles while e3, f3 and e5 represents biarticular muscles. The pairs e1-f1, e2-f2, e3-f3 and e4-f4 works in coordination and generates a torque on the joints which they are connected to. Monoarticular muscles #1,#2 and #4 generate a torque only one joint, while biarticular muscles #3 and #5 generate torques on two adjacent joints and the resulted torques can be shown as:

$$\begin{aligned} T_1 &= (e_1 - f_1)r_j \\ T_2 &= (e_2 - f_2)r_j \\ T_3 &= (e_3 - f_3)r_j \\ T_4 &= (e_4 - f_4)r_j \\ T_5 &= e_5 r_j \end{aligned} \qquad \text{(Eq. 3.1)}$$

where T_i denotes individual muscle torques and r_j denotes the radius of joints

3.2 Explanation of Robotic Leg Motion

The motion of the leg is analyzed in two schemes, one is the state expressed by ‘legon’ and the other is expressed by ‘legoff’. The notation ‘legon’ will be used for the leg which contacts with the ground while walking and the notation ‘legoff’ will be used for the leg which does not contact with the ground and taking one step forward.

3.2.1 General Scheme of Walking

The trajectories of hip and ankle joints are thought to be arc-like which is close to human motion. In the legon state, it is considered that the angle of knee joint is fixed to some value and hip trajectory is calculated according to that given value. The trajectories for legoff state is adjusted according to the trajectory of legon state in order to sync the motion of both legs. For the legoff state, horizontal travel distance of the ankle is designed to be two times of the horizontal travel distance of hip so that when the leg which is in contact with the ground finishes its move, the other leg will just contact the ground. This process continues repeatedly as the robot moves forward. The trajectories for both states is shown in the Figure 3.3 below

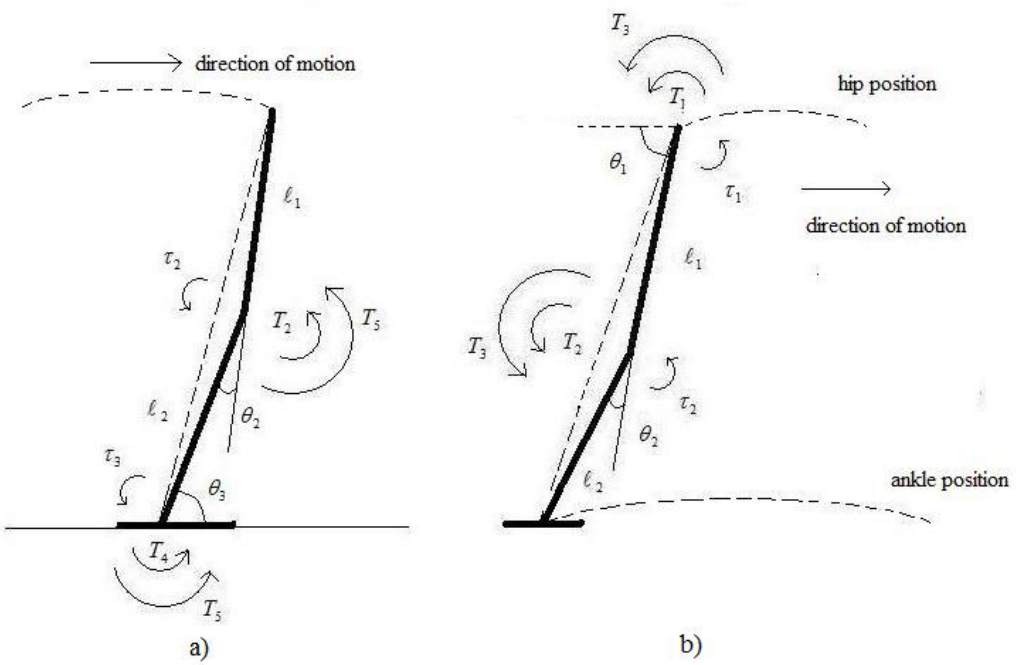

Figure 3.3 Trajectories for a)legon state b) legoff state

In this figure; the total torques generated at joints can be expressed as;

$$\begin{bmatrix} \tau_3 \\ \tau_2 \end{bmatrix} = \begin{bmatrix} T_4 + T_5 \\ T_2 + T_5 \end{bmatrix} \qquad \text{(Eq. 3.2)}$$

$$\begin{bmatrix} \tau_2 \\ \tau_1 \end{bmatrix} = \begin{bmatrix} T_2 + T_3 \\ T_1 + T_3 \end{bmatrix} \qquad \text{(Eq. 3.3)}$$

where τ_1 is the hip torque, τ_2 is the knee torque, τ_3 is the ankle torque, T_1, T_2, T_4 are monoarticular muscle torques and T_3, T_5 are biarticular muscle torques.

3.2.2 Trajectory Planning

Trajectory of the hip is designed as a cubic polynomial where it is needed to input initial and final positions, initial and final velocities and the travel time. The reason why cubic polynomial is chosen is that, it is required to have five parameters in order to adjust for all initial and final positions, velocities and travel time. The 3rd order polynomial trajectory for x-position for legon state is expressed as;

$$q_x = a_0 + a_1 t + a_2 t^2 + a_3 t^3$$
$$\dot{q}_x = a_1 + 2a_2 t + 3a_3 t^2$$

$$a_0 = q_i \qquad \text{(Eq. 3.4)}$$
$$a_1 = \dot{q}_i$$
$$a_2 = \frac{3(q_f - q_i) - (2\dot{q}_i + \dot{q}_f)t_f}{{t_f}^2}$$
$$a_3 = \frac{2(q_i - q_f) + (\dot{q}_i + \dot{q}_f)t_f}{{t_f}^3}$$

where q_x is the x-position of the hip, $\dot{q}_x$ is the x-velocity of the hip, q_i is the initial position, q_f is the final position, $\dot{q}_i$ is the initial velocity, $\dot{q}_f$ is the final velocity and t_f is the total travel time.

For the case which knee joint angle is fixed, z-position is calculated according the x-position in order to guarantee that the knee angle would be fixed. So the equation for z-position becomes,

$$q_z = L\sin(\cos^{-1}(q_x / L)) \qquad \text{(Eq. 3.5)}$$

where L is the distance from ankle to hip and can be expressed by,

$$L = \sqrt{{\ell_1}^2 + {\ell_2}^2 + 2\ell_1\ell_2\cos(\theta_2)} \qquad \text{(Eq. 3.6)}$$

3.2.3 Calculations of Angles, Angular Velocities, Angular Accelerations and Joint Torques

After generating the trajectory, it is required to calculate each joint angles, angular velocities and angular accelerations for calculating the needed joint torques. Inverse kinematics solution is used to get each angles for the given trajectory. Since a time profile is also set in the trajectory planning step, it

becomes easy to calculate each angular velocities and angular accelerations by taking direct derivatives of angle equation.

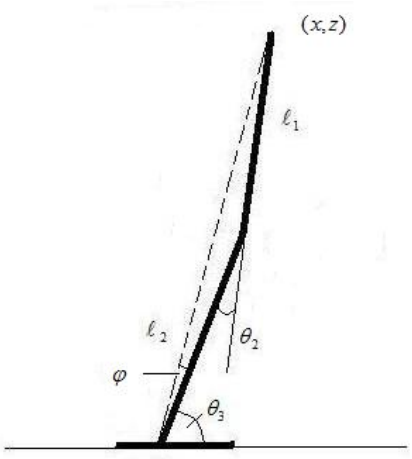

Figure 3.4 Robotic leg model for inverse kinematics

Equations for inverse kinematics solution are,

$$\begin{aligned}
\theta_2 &= \mp 2\tan^{-1}\sqrt{\frac{(\ell_1+\ell_2)^2-(x^2+z^2)}{(x^2+z^2)-(\ell_1-\ell_2)^2}} \\
\phi &= \tan^{-1}(z,x) \\
\varphi &= \tan^{-1}(\ell_2\sin\theta_2, \ell_1+\ell_2\cos\theta_2) \\
\theta_3 &= \phi \mp \varphi
\end{aligned} \qquad \text{(Eq. 3.7)}$$

The position matrix for hip can be expressed by,

$$\begin{bmatrix} x \\ z \end{bmatrix} = \begin{bmatrix} \ell_1\cos(\theta_2+\theta_3)+\ell_2\cos\theta_3 \\ \ell_1\sin(\theta_2+\theta_3)+\ell_2\sin\theta_3 \end{bmatrix} \qquad \text{(Eq. 3.8)}$$

and Jacobian Matrix J can be calculated directly from position matrix as,

$$J = \begin{bmatrix} -\ell_1\sin(\theta_2+\theta_3) & -\ell_1\sin(\theta_2+\theta_3)-\ell_2\sin(\theta_3) \\ \ell_1\cos(\theta_2+\theta_3) & \ell_1\cos(\theta_2+\theta_3)+\ell_2\cos(\theta_3) \end{bmatrix} \qquad \text{(Eq.3.9)}$$

The general torque equation is defined as;

$$\tau = D(\theta)\ddot{\theta} + C(\theta,\dot{\theta})\dot{\theta} + g(\theta) \qquad \text{(Eq.3.10)}$$

where $D(\theta)$ is the Inertia matrix, $C(\theta,\dot{\theta})$ is the Coriolis matrix and $g(\theta)$ is the gravitational effect.

The links of the robotic leg is considered to be cylindrical shape as seen in the Figure 3.5

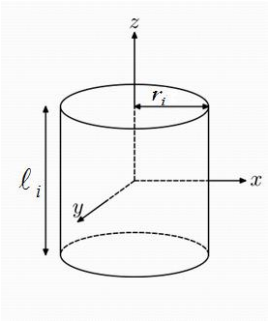

Figure 3.5 Simplified representation of robotic leg links

The inertia of the links are expressed as;

$$I_i = m_i\left(\frac{r_i^{\,2}}{4} + \frac{\ell_i^{\,2}}{12}\right) \qquad \text{(Eq. 3.11)}$$

where m_i is the mass of links, r_i is the radius of cylinder and ℓ_i is the length of links.

If matrix form is used to represent the torque equation for legon state, the representation will be,

$$\begin{bmatrix}\tau_3\\ \tau_2\end{bmatrix} = \begin{bmatrix}d_{11} & d_{12}\\ d_{21} & d_{22}\end{bmatrix}\begin{bmatrix}\ddot{\theta}_3\\ \ddot{\theta}_2\end{bmatrix} + \begin{bmatrix}c_{11} & c_{12}\\ c_{21} & c_{22}\end{bmatrix}\begin{bmatrix}\dot{\theta}_3\\ \dot{\theta}_2\end{bmatrix} + \begin{bmatrix}g_1\\ g_2\end{bmatrix} \qquad \text{(Eq. 3.12)}$$

where,

$$\begin{aligned}
d_{11} &= m_2\ell_{c2}^{\,2} + m_1(\ell_2^{\,2} + \ell_{c1}^{\,2} + 2\ell_2\ell_{c1}\cos\theta_2) + I_1 + I_2\\
d_{12} &= d_{21} = m_1(\ell_{c1}^{\,2} + \ell_2\ell_{c1}\cos\theta_2) + I_1\\
d_{22} &= m_1\ell_{c1}^{\,2} + I_1
\end{aligned}$$

$$\begin{aligned}
c_{11} &= -(m_1\ell_2\ell_{c1}\sin\theta_2)\dot{\theta}_2\\
c_{12} &= -(m_1\ell_2\ell_{c1}\sin\theta_2)(\dot{\theta}_2 + \dot{\theta}_3)\\
c_{21} &= (m_1\ell_2\ell_{c1}\sin\theta_2)\dot{\theta}_3\\
c_{22} &= 0
\end{aligned} \qquad \text{(Eq. 3.13)}$$

$$\begin{aligned}
g_1 &= (m_2\ell_{c2} + m_1\ell_2)g\cos\theta_3 + m_1.\ell_{c1}g\cos(\theta_2 + \theta_3)\\
g_2 &= m_1\ell_{c1}g\cos(\theta_2 + \theta_3)
\end{aligned}$$

In legon state, the resulted joint torques for ankle and knee becomes;

$$\begin{aligned}\tau_3 &= (m_2\ell_{c2}{}^2 + m_1(\ell_2{}^2 + \ell_{c1}{}^2 + 2\ell_2\ell_{c1}\cos\theta_2) + I_1 + I_2)\ddot{\theta}_3 \\ &+ (m_1(\ell_{c1}{}^2 + \ell_1\ell_{c1}\cos(\theta_2)) + I_1)\ddot{\theta}_2 - m_1\ell_2\ell_{c1}\sin(\theta_2)(2\ddot{\theta}_2\dot{\theta}_3 + \ddot{\theta}_2{}^2) \\ &+ (m_2\ell_{c2} + m_1\ell_2)g\cos\theta_3 + m_1\ell_{c1}g\cos(\theta_2+\theta_3)\end{aligned} \quad \text{(Eq. 3.14)}$$

$$\begin{aligned}\tau_2 &= (m_1(\ell_{c1}{}^2 + \ell_2\ell_{c1}\cos\theta_2) + I_1)\ddot{\theta}_3 + (m_1\ell_2\ell_{c1}\sin\theta_2)\dot{\theta}_3 \\ &+ (m_1\ell_{c1}{}^2 + I_1)\ddot{\theta}_2 + m_1\ell_2\ell_{c1}\sin(\theta_2)(\dot{\theta}_3{}^2 + \dot{\theta}_2\dot{\theta}_3) + m_1\ell_{c1}g\cos(\theta_2+\theta_3)\end{aligned} \quad \text{(Eq.3.15)}$$

In legoff state, the resulted joint torques for hip and knee becomes;

$$\begin{aligned}\tau_1 &= (m_1\ell_{c1}{}^2 + m_2(\ell_1{}^2 + \ell_{c2}{}^2 + 2\ell_1\ell_{c2}\cos\theta_2) + I_1 + I_2)\ddot{\theta}_1 \\ &+ (m_2(\ell_{c2}{}^2 + \ell_1\ell_{c2}\cos\theta_2) + I_2)\ddot{\theta}_2 - (m_2\ell_1\ell_{c2}\sin\theta_2)(2\dot{\theta}_1 + \dot{\theta}_2)\dot{\theta}_2 \\ &- (m_1\ell_{c1} + m_2\ell_1)g\cos\theta_3 - m_2\ell_{c2}g\cos(\theta_1+\theta_2)\end{aligned} \quad \text{(Eq. 3.16)}$$

$$\begin{aligned}\tau_2 &= (m_2(\ell_{c2}{}^2 + \ell_1\ell_{c2}\cos\theta_2) + I_2)\ddot{\theta}_1 + (m_2\ell_{c2}{}^2 + I_2)\ddot{\theta}_2 \\ &+ (m_2\ell_1\ell_{c2}\sin\theta_2)(\dot{\theta}_1 + \dot{\theta}_2)\dot{\theta}_1 - m_2\ell_{c2}g\cos(\theta_1+\theta_2)\end{aligned} \quad \text{(Eq. 3.17)}$$

3.2.4 Calculations of Individual Muscle Torques

In the muscle mechanism, there is actuator redundancy since the number of actuators are more than the number of joints. For each state, legon and legoff, there are 2 joint torques which should be shared by 3 different muscle torques. In this research, in order to solve that problem 2-norm approach is used. For legon state, joint torques in matrix form can be expressed as;

$$\begin{bmatrix}\tau_2 \\ \tau_3\end{bmatrix} = \begin{bmatrix}T_2 + T_5 \\ T_4 + T_5\end{bmatrix} \quad \text{(Eq. 3.18)}$$

By minimizing $\sqrt{T_2{}^2 + T_4{}^2 + T_5{}^2}$, the resulted individual muscle torques become;

$$T_2 = \frac{(\tau_3 - \tau_2)T_{2,\max}{}^2 T_{5,\max}{}^2 + \tau_3 T_{2,\max}{}^2 T_{4,\max}{}^2}{T_{2,\max}{}^2 T_{5,\max}{}^2 + T_{2,\max}{}^2 T_{4,\max}{}^2 + T_{4,\max}{}^2 T_{5,\max}{}^2} \quad \text{(Eq. 3.19)}$$

$$T_4 = \frac{\tau_2 T_{2,\max}{}^2 T_{4,\max}{}^2 + (\tau_2 - \tau_3)T_{4,\max}{}^2 T_{5,\max}{}^2}{T_{2,\max}{}^2 T_{5,\max}{}^2 + T_{2,\max}{}^2 T_{4,\max}{}^2 + T_{4,\max}{}^2 T_{5,\max}{}^2} \quad \text{(Eq. 3.20)}$$

$$T_5 = \frac{\tau_3 T_{4,\max}{}^2 T_{5,\max}{}^2 + \tau_2 T_{2,\max}{}^2 T_{5,\max}{}^2}{T_{2,\max}{}^2 T_{5,\max}{}^2 + T_{2,\max}{}^2 T_{4,\max}{}^2 + T_{4,\max}{}^2 T_{5,\max}{}^2} \quad \text{(Eq. 3.21)}$$

where $T_{i,\max}$ denotes the maximum torque that muscle can generate.

The proof of equations 3.19-20-21 is provided in Appendix A.

If the maximum torques of all muscles are same $T_{2,\max} = T_{4,\max} = T_{5,\max}$ the solution becomes simpler as;

$$\begin{aligned} T_2 &= -\frac{1}{3}\tau_3 + \frac{2}{3}\tau_2 \\ T_4 &= \frac{2}{3}\tau_3 - \frac{1}{3}\tau_2 \\ T_5 &= \frac{1}{3}\tau_3 + \frac{1}{3}\tau_2 \end{aligned} \qquad \text{(Eq. 3.22)}$$

Since T_5 can generate torque only in one direction, it is required to update it as;

If T_5 <0

$$\begin{aligned} T_2^* &= T_2 + T_5 \\ T_4^* &= T_4 + T_5 \\ T_5^* &= 0 \end{aligned} \qquad \text{(Eq. 3.23)}$$

otherwise

$$\begin{aligned} T_2^* &= T_2 \\ T_4^* &= T_4 \\ T_5^* &= T_5 \end{aligned} \qquad \text{(Eq. 3.24)}$$

By applying the same principles to legoff state and minimize $\sqrt{T_1^{\,2} + T_2^{\,2} + T_3^{\,2}}$, solution becomes;

$$\begin{aligned} T_1 &= \frac{2}{3}\tau_1 - \frac{1}{3}\tau_2 \\ T_2 &= -\frac{1}{3}\tau_1 + \frac{2}{3}\tau_2 \\ T_3 &= \frac{1}{3}\tau_1 + \frac{1}{3}\tau_2 \end{aligned} \qquad \text{(Eq. 3.25)}$$

3.3 The Effect of External Forces

The calculations for muscle torques in order to move the robotic leg in the previously designed trajectory are shown until this point; but there might also be some external forces acting on the body such as a mass can be put on the body, somebody may just exert a force on the body, etc. as seen in the Figure 3.6 below. In order to reject the effect of such forces it is needed to include their effects into the torque calculations.

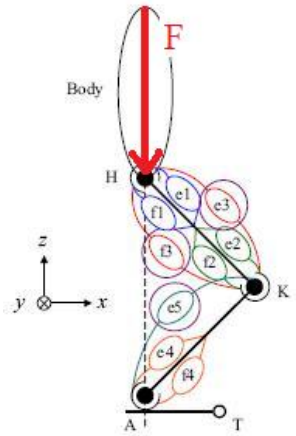

Figure 3.6 External force acting on body

The relation between torque and the end effector force is given as;

$$T = -J^T F \qquad \text{(Eq.3.26)}$$

For legon state, knee torque τ_2 and ankle torque τ_3 becomes;

$$\begin{bmatrix} \tau_3 \\ \tau_2 \end{bmatrix} = \begin{bmatrix} \ell_1 \sin(\theta_2+\theta_3) & -\ell_1 \cos(\theta_2+\theta_3) \\ \ell_1 \sin(\theta_2+\theta_3)+\ell_2 \sin(\theta_3) & -\ell_1 \cos(\theta_2+\theta_3)-\ell_2 \cos(\theta_3) \end{bmatrix} \begin{bmatrix} F_x \\ F_z \end{bmatrix} \qquad \text{(Eq.3.27)}$$

3.3.1 External Force Rejection Strategy

The external force acting on the body is divided into two components, one is in the direction from hip position to ankle position, the other is perpendicular to that direction. In order to do that, the angle α is assigned for the angle between the direction from hip to ankle and the direction of the force acting on the body as it is seen in the Figure3.7 Zw-Xw is the world coordinate and Xr-Zr is the robot coordinate.

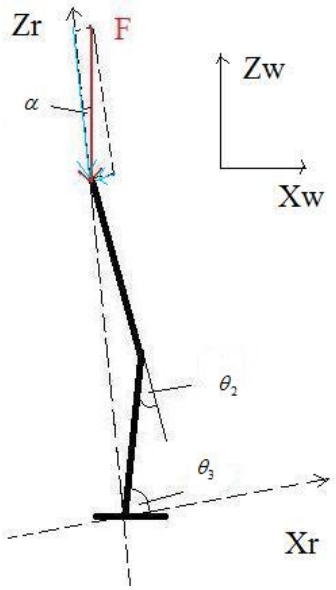

Figure 3.7 External force components and coordinate representation

α and components of external force F are given as;

$$\alpha = \theta_3 + \frac{\theta_2}{2} - \frac{\pi}{2} \quad \text{(Eq. 3.28)}$$

$$F_{parallel} = F\cos\alpha$$
$$F_{perpendicular} = F\sin\alpha \quad \text{(Eq. 3.29)}$$

$F_{parallel}$ will be rejected by muscles #1, #2 and #3 and $F_{perpendicular}$ will be rejected by muscles #2, #4 and #5.

$$\begin{bmatrix}\tau_{1ex}\\ \tau_{2ex}\end{bmatrix} = \begin{bmatrix}T_1 + T_3\\ T_2 + T_3\end{bmatrix} = \begin{bmatrix}0\\ F\ell\cos\alpha\sin(\theta_2/2)\end{bmatrix} \quad \text{(Eq. 3.30)}$$

where $T_3 = -T_1 = T$ and link lengths $\ell_1 = \ell_2 = \ell$

When this external torque is shared by muscles #1, #2 and #3, the total torque according to muscle #2 torque, is shown in Figure 3.8. It can be said from this figure that, for total torque efficiency, T_2 is required to be as high as possible. When T_2 torque is above maximum torque that muscle #2 can generate, then T_3 and T_1 should be activated.

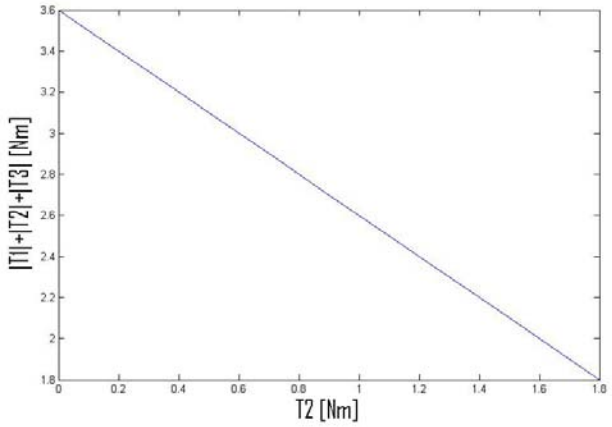

Figure 3.8 Total muscle torques vs. T2 torque

If $F_{perpendicular}$ is expressed in the world coordinates, transformation would be

$$\begin{bmatrix}F_{px}\\ F_{pz}\end{bmatrix} = \begin{bmatrix}\cos\alpha & -\sin\alpha\\ \sin\alpha & \cos\alpha\end{bmatrix}\begin{bmatrix}F\sin\alpha\\ 0\end{bmatrix} \quad \text{(Eq. 3.31)}$$

$$\begin{bmatrix}F_{px}\\ F_{pz}\end{bmatrix} = \begin{bmatrix}F\cos\alpha\sin\alpha\\ F\sin^2\alpha\end{bmatrix} \quad \text{(Eq. 3.32)}$$

The resulted torque on knee joint and ankle joint becomes;

$$\begin{bmatrix} \tau_{3ex} \\ \tau_{2ex} \end{bmatrix} = \begin{bmatrix} \ell_1 \sin(\theta_2+\theta_3) & -\ell_1 \cos(\theta_2+\theta_3) \\ \ell_1 \sin(\theta_2+\theta_3)+\ell_2 \sin(\theta_3) & -\ell_1 \cos(\theta_2+\theta_3)-\ell_2 \cos(\theta_3) \end{bmatrix} \begin{bmatrix} F_{px} \\ F_{pz} \end{bmatrix} \quad \text{(Eq. 3.33)}$$

3.3.2 The Advantage of using Biarticular Muscle in External Force Rejection

As the characteristics of monoarticular and biarticular muscles are explained in detail in Chapter 2.4, the magnitude of end point force in the direction from ankle to hip is bigger for small knee angles. The response to high external force in vertical direction is expected to be better and more external force can be rejected in compared to conventional model. Additionally, biarticular muscles help robotic leg to keep its posture, especially in x-direction. Detailed analysis will be shown in Chapter 4.3.2

3.4 Muscle Control Method

In human leg muscles, muscle torque is adjusted by tightening or loosening the muscle itself. In order to have very similar characteristics to human leg muscle, it is thought to use a spring-damper system and a DC motor to change the length of the muscle so that a torque would be produced on the hip, knee and ankle joints. By changing the length of the muscle, position and force control is tried to be achieved. In this system, rotational motion of DC motor is converted to translational motion and a force is acted on the edge of joints.

3.4.1 The Representation of Muscle Model

The muscle model that is used in this research is shown in the Figure3.9 below.

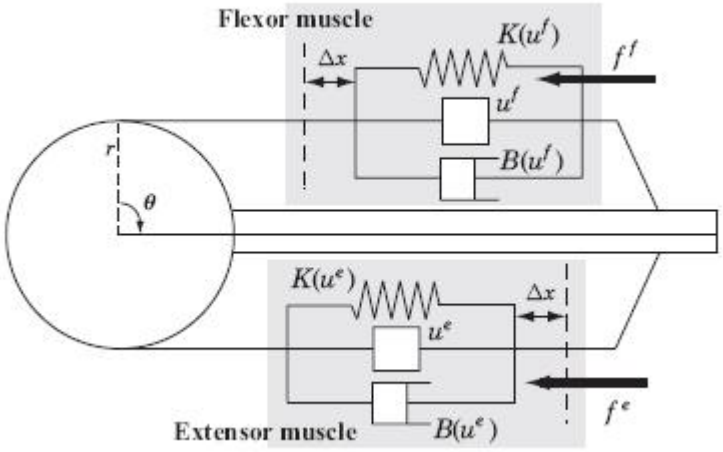

Figure 3.9 Muscle model

In this model because of the change in muscle length, a force is acting on the edge of joint and that force can be represented as follows,

$$f^{e,f} = m\Delta\ddot{x} + K\Delta x + B\Delta\dot{x} \quad \text{(Eq. 3.34)}$$

where $f^{e,f}$ is the force acted on the joint, m is the mass of the system, K is the spring constant and B is the damping coefficient of the muscle. According to the direction of muscle torques, it is decided which one of extensor or flexor would be stretched as given in equations 3.35 to 3.43

if T_1<0
$$f_1^{\,e} = T_1 / r_j \qquad f_1^{\,f} = 0 \qquad \text{(Eq. 3.35)}$$

otherwise
$$f_1^{\,e} = 0 \qquad f_1^{\,f} = T_1 / r_j \qquad \text{(Eq. 3.36)}$$

if T_2<0
$$f_2^{\,e} = T_2 / r_j \qquad f_2^{\,f} = 0 \qquad \text{(Eq. 3.37)}$$

otherwise
$$f_2^{\,e} = 0 \qquad f_2^{\,f} = T_2 / r_j \qquad \text{(Eq. 3.38)}$$

if T_3<0
$$f_3^{\,e} = T_3 / r_j \qquad f_3^{\,f} = 0 \qquad \text{(Eq. 3.39)}$$

otherwise
$$f_3^{\,e} = 0 \qquad f_3^{\,f} = T_3 / r_j \qquad \text{(Eq. 3.40)}$$

if T_4<0
$$f_4^{\,e} = T_4 / r_j \qquad f_4^{\,f} = 0 \qquad \text{(Eq. 3.41)}$$

otherwise
$$f_4^{\,e} = 0 \qquad f_4^{\,f} = T_4 / r_j \qquad \text{(Eq. 3.42)}$$

$$f_5^{\,e} = T_5 / r_j \qquad \text{(Eq. 3.43)}$$

3.4.2 Calculation of Muscle Displacement

After calculations of individual muscle forces, the next step is to calculate the required muscle displacements which then will be used as reference for DC motor position control under external torque. The relation between muscle displacement x and muscle force f is expressed as follows;

$$f = m\Delta\ddot{x} + K\Delta x + B\Delta\dot{x} \qquad \text{(Eq. 3.44)}$$

$$f_{monoarticular} = m(\ddot{x} - r\ddot{\theta}) + K(x - r.\theta) + B(\dot{x} - r.\dot{\theta}) \qquad \text{(Eq. 3.45)}$$

$$f_{biarticular} = m(\ddot{x} - r(\ddot{\theta}_1 + \ddot{\theta}_2)) + K(x - r(\theta_1 + \theta_2)) + B(\dot{x} - r(\dot{\theta}_1 + \dot{\theta}_2)) \qquad \text{(Eq. 3.46)}$$

where $x = r\theta$ for monoarticular muscles since they are connected to only one joint, and $x = r(\theta_1 + \theta_2)$ for biarticular muscles since they are connected to two adjacent joints.

3.4.3 The method to control with DC Motor

Previously calculated muscle displacements are used as a reference for DC motor and the rotational motion of DC motor is converted to translational motion by the use of a wire system. Individual muscle torques are considered to be external torques that opposes the rotational motion of DC motor. In order to reject such disturbance, disturbance observer is decided to be used in order to estimate resulted torque errors and used as a feedback.

3.4.4 Control Diagram

For DC motor controller, it is required to control the length of the muscle which is achieved by turning the DC motor and translating the rotational motion into translational motion. Since there would also be external torque which is individual muscle torque, it is needed to compensate the effect of that external disturbance.

Basic representation of the disturbance observer that is used in DC motor position control is shown in Figure 3.10 below.

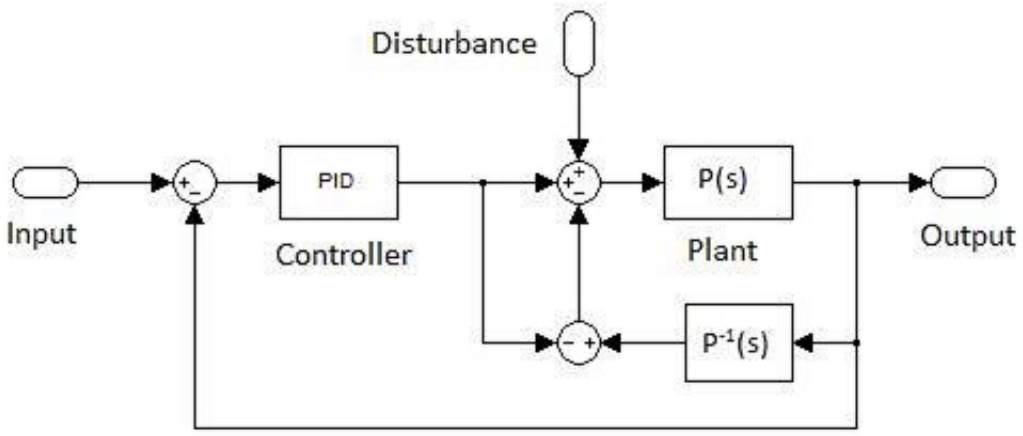

Figure 3.10 Disturbance observer

By using disturbance observer, the difference between output torque and input torque is given to the system as feedback which results in better performance of disturbance rejection. Details of the Control Diagram is shown in Appendix B.

The representation of DC motor that is used for muscle force generation is shown in Figure 3.11

Equations for armature side and rotor side are as follows

$$J\ddot{\theta} + b\dot{\theta} = K_t i(t)$$
$$L\frac{di(t)}{dt} + Ri(t) = V - K_e\dot{\theta} \qquad \text{(Eq. 3.47)}$$

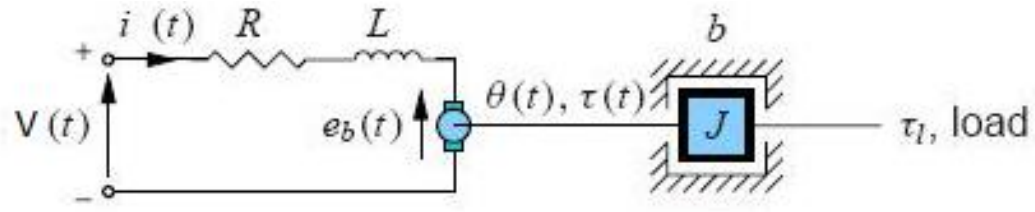

Figure 3.11 DC motor model

Laplace transformations can be written as;

$$(Js^2 + bs)\theta(s) = K_t I(s)$$
$$(Ls + R)I(s) = V - K_e s\theta(s) \quad \text{(Eq. 3.48)}$$

$$\frac{\theta(s)}{V} = \frac{K_t}{JLs^3 + (JR + bL)s^2 + (K_e K_t + bR)s} \quad \text{(Eq. 3.49)}$$

This model is applied for control of both conventional model and muscle model. The difference is that, in conventional model joint angle is taken directly as position reference and joint torques is taken as external torques. In muscle model, muscle displacements are taken as position reference and individual muscle torques are considered to be external torques. The output position is used to estimate each joint angles.

3.5 Output Angle Calculations

The output torque of the system is used to estimate the angular deflection on joints. For legon state, the relation between muscle torque error and angular deflections resulted from torque error can be expressed as,

$$\tau = (m\ddot{x} + B\dot{x} + Kx)r \quad \text{(Eq. 3.50)}$$

$$\Delta\tau_{m4} = (mr\Delta\ddot{\theta}_3 + Br\Delta\dot{\theta}_3 + Kr\Delta\theta_3)r \quad \text{(Eq. 3.51)}$$

$$\Delta\tau_{m2,m3} = (mr\Delta\ddot{\theta}_2 + Br\Delta\dot{\theta}_2 + Kr\Delta\theta_2)r \quad \text{(Eq. 3.52)}$$

$$\Delta\tau_{m5} = (mr(\Delta\ddot{\theta}_2 + \Delta\ddot{\theta}_3)) + Br(\Delta\dot{\theta}_2 + \Delta\dot{\theta}_3) + Kr(\Delta\theta_2 + \Delta\theta_3)r \quad \text{(Eq. 3.53)}$$

where $m2, m3, m4$ and $m5$ represents the muscles #2,#3,#4 and #5 respectively. The total torques on knee joint and ankle joint becomes,

$$\Delta\tau_{knee} = \Delta\tau_{m2} + \Delta\tau_{m3} + \Delta\tau_{m5} \quad \text{(Eq. 3.54)}$$

$$\Delta\tau_{ankle} = \Delta\tau_{m4} + \Delta\tau_{m5} \quad \text{(Eq. 3.55)}$$

Solving those equations for $\Delta\theta_2$ and $\Delta\theta_3$ on MATLAB/Simulink environment gives the angular deflections on joints.

3.6 Summary of Chapter

Theoretical and mathematical representations of robotic leg with muscle model are provided in detail. After giving the outline of the robotic leg motion, walking scheme, trajectory planning, calculations for angles, angular velocities, angular accelerations and joint torques are presented. The method to calculate individual muscle torques from joint torques is explained. Moreover, the effect of external forces on joint torques is given and the strategy to reject that force is explained. Resulted muscle displacement calculations are shown and the method to control each muscle torque is discussed. Finally, control diagram for muscles is provided.

Chapter 4

Simulation Results for Different External Forces in Conventional Model and Muscle Model

In this chapter, the motion of both legs is simulated in MATLAB/Simulink environment with the use of mathematical modeling that is given in the previous chapter. Two different schemes are considered, one is the conventional type robotic leg and the other is the robotic leg with monoarticular and biarticular muscle mechanism. First, given parameters for the simulation will be shown and then performance comparison in terms of failure conditions, position tracking and maximum external force rejection capability will be given for different situations.

4.1 Simulation Model, Assumptions, Tables of Given Values, Motor Characteristics

For simulations, the motion of the leg which is in contact with the ground is considered to be rotating around its ankle joint from 95 degrees to 75 degrees from left to right as seen in Figure 4.1

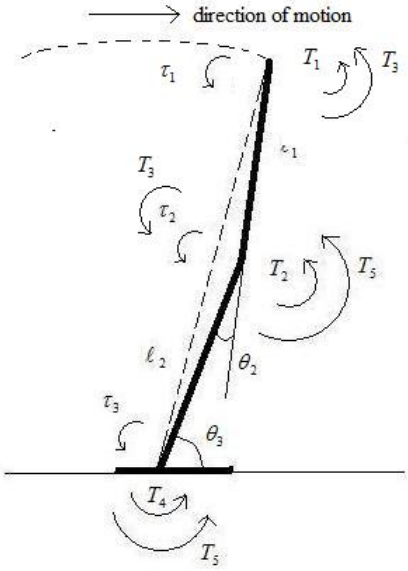

Figure 4.1 Robotic leg 'legon' motion

Walking step size is considered to be small to achieve balance easier for the robotic leg. The values given for link lengths, masses and the radius of the links are shown in Table4.1, the motor parameters used in the simulations are shown in Table4.2 The motor used in simulation is Maxon RE40 DC Motor.

Table4.1 Table of given values

m_1, m_2	mass of links	3 kg
ℓ_1, ℓ_2	length of links	0.2 m
θ_2	knee angle	0.1745rad(Case1)
r	radius of links	0.03 m

Table4.2 Table of motor parameters

Parameters	Explanation	Value	Units
J	inertia	1.34E-5	Kg-m^2/rad
b	damping coefficient	3.5077E-6	N-m/(rad/s)
K_e	back-emf constant	0.0302	Volt/(rad/s)
K_t	torque constant	0.0302	N-m/A
L	inductance	0.08	mH
R	resistance	0.316	Ohm

4.2 Trajectories for Simulation

Simulation results will be shown for two methods in two different cases. In the first case (Case1), the knee angle is decided to be fixed and the trajectory of the hip is designed accordingly by using cubic trajectory generation. In the second case (Case2), the knee angle is not fixed and the hip trajectory is designed in a such a way that the robot moves with constant horizontal velocity and keeps its height at same level. The trajectories and joint angles for both Case1 and Case2 are shown in Figures 4.2 and Figure 4.3, respectively.

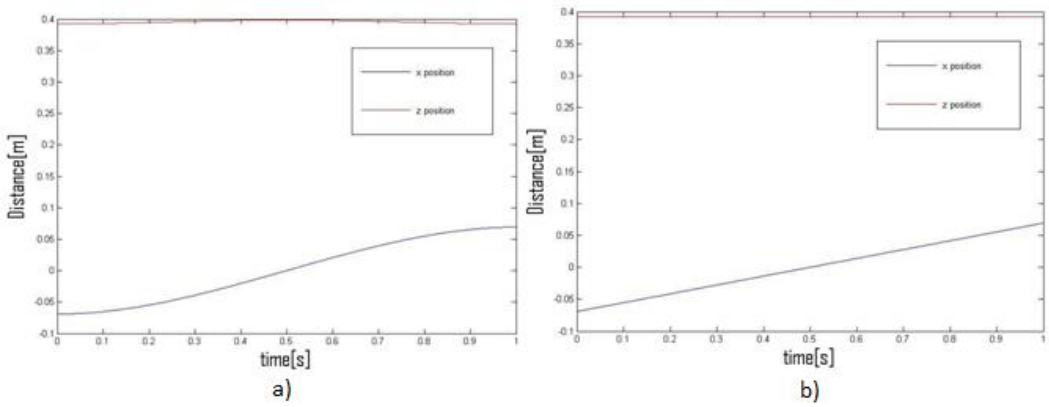

Figure 4.2 Trajectory of hip position for a)case1 b)case2

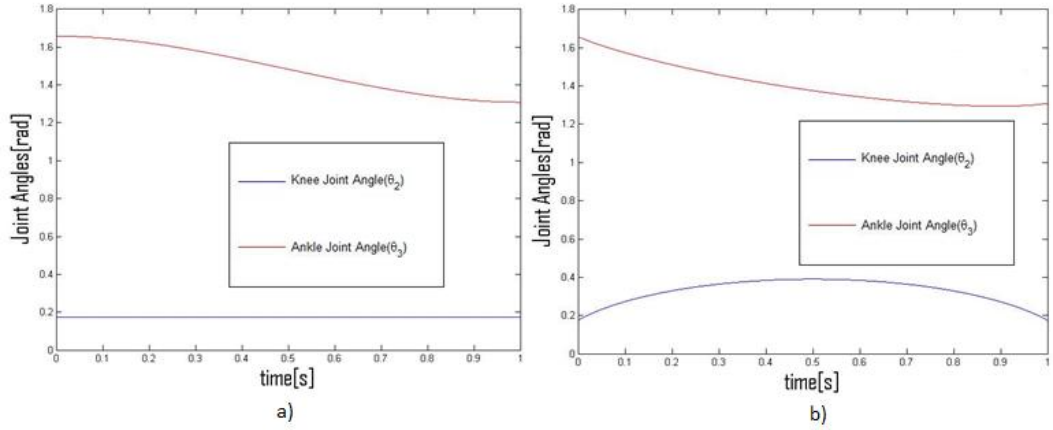

Figure 4.3 Joint angles in legon state for a)case1 b)case2

The trajectory of second leg is generated according to the trajectory of the first leg. Second leg, which is the leg in legoff state, lefts the ground and moves up to 1 cm and steps forward and touch the ground at the end of its motion. The motion of robotic legs in two cases can be seen in Figure 4.4, resulted joint torques are shown in Figure 4.5 below.

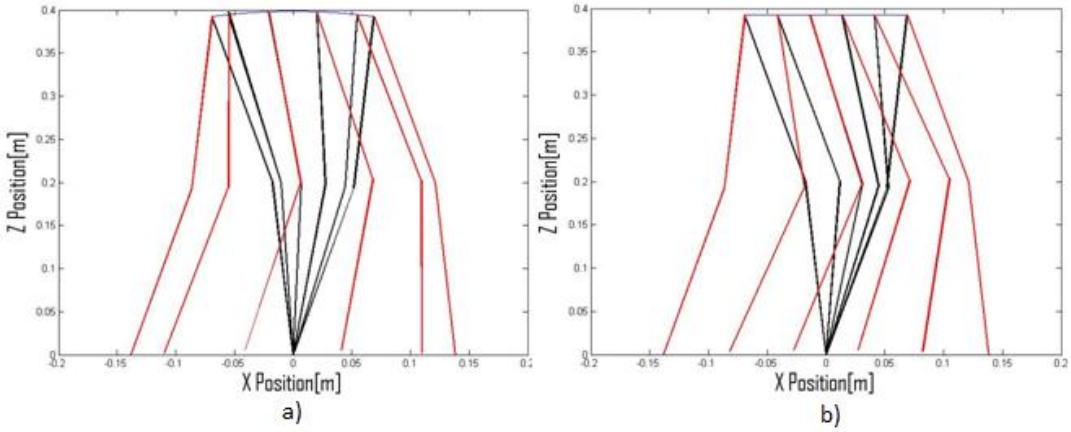

Figure 4.4 Robotic leg motions for a)case1 b)case2

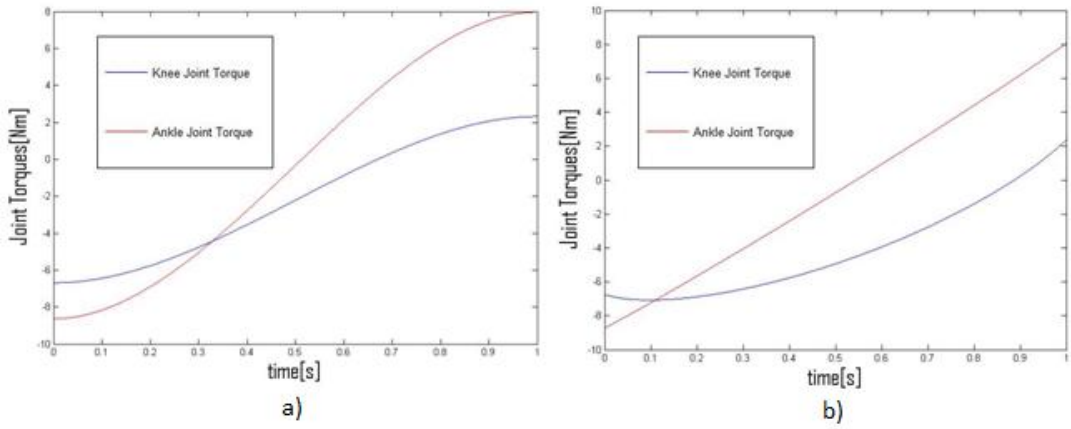

Figure 4.5 Joint torques in legon state for a)case1 b)case2

4.3 Performance Comparison between Conventional Method and Muscle Method

In this section, two different methods, conventional model vs. muscle model, are simulated and compared in terms of their maximum external force rejection capabilities, tracking performances and the self-stability in case of using biarticular muscle or not.

4.3.1 Performance of Muscle Torque Generation

In the conventional method, angular position control is implemented by DC motors that are placed on joints. The torque which opposes the rotational motion of the motor is rejected by the help of a torque observer. The total torque that can be produced on the joints is limited by the maximum torque that DC motor can generate.

But in the muscle model, since the total torque is shared by more actuators, the maximum torque that can be produced on the joints is higher in compared to conventional method. The total torque of the actuators in case of using biarticular muscle can also be reduced in compared to using only monoarticular muscles. The following example represents the advantage of using biarticular muscle.

For Conventional Method;

$$\begin{bmatrix} \tau_1 \\ \tau_2 \end{bmatrix} = \begin{bmatrix} T_1 \\ T_2 \end{bmatrix} \quad \text{(Eq. 4.1)}$$

$$T_1 + T_2 = \tau_1 + \tau_2 \quad \text{(Eq. 4.2)}$$

For Mono-Mono Configuration;

$$\begin{bmatrix} \tau_1 \\ \tau_2 \end{bmatrix} = \begin{bmatrix} T_1 + T_2 \\ T_3 + T_4 \end{bmatrix} \quad \text{(Eq. 4.3)}$$

$$T_1 + T_2 + T_3 + T_4 = \tau_1 + \tau_2 \quad \text{(Eq. 4.4)}$$

For Mono-Bi Configuration;

$$\begin{bmatrix} \tau_1 \\ \tau_2 \end{bmatrix} = \begin{bmatrix} T_1 + T_3 \\ T_2 + T_3 \end{bmatrix} \quad \text{(Eq. 4.5)}$$

$$T_1 + T_2 + T_3 = \frac{2}{3}(\tau_1 + \tau_2) \quad \text{(Eq. 4.6)}$$

where

$$T_1 = \frac{2}{3}\tau_1 - \frac{1}{3}\tau_2$$
$$T_2 = -\frac{1}{3}\tau_1 + \frac{2}{3}\tau_2 \qquad \text{(Eq. 4.7)}$$
$$T_3 = \frac{1}{3}\tau_1 + \frac{1}{3}\tau_2$$

In case of using actuators with the same maximum torques, the total maximum torque of actuators are $2\tau_{max}$ for conventional, $4\tau_{max}$ mono-mono configuration and $3\tau_{max}$ for mono-bi configuration. To achieve same total torques, the maximum torque of each actuator is reduced to $\frac{1}{2}\tau_{max}$ for mono-mono configuration and $\frac{2}{3}\tau_{max}$ for mono-bi configuration. The resultant maximum torques at each joint becomes $2\tau_{max}$ for all configurations. The comparison of these three configurations in case of equal total actuator torque is shown in Table 4.3a. Moreover if we adjust the maximum torques of each actuators in a such a way that the maximum possible torque at each joint would be τ_{max}, the resultant total actuator torques become $2\tau_{max}$ for conventional and mono-mono configuration, and $\frac{3}{2}\tau_{max}$ for mono-bi configuration. Comparison is shown in Table 4.3b In these two cases, it can be said that mono-bi configuration is better to other two configurations.

Table 4.3a Comparisons of different configurations in case of same actuator torque

	maximum possible joint torque	total actuator torque
conventional	τ_{max}	$2\tau_{max}$
mono-mono	τ_{max}	$2\tau_{max}$
mono-bi	$\frac{4}{3}\tau_{max}$	$2\tau_{max}$

Table 4.3b Comparisons of different configurations in case of same maximum possible joint torque

	maximum possible joint torque	total actuator torque
conventional	τ_{max}	$2\tau_{max}$
mono-mono	τ_{max}	$2\tau_{max}$
mono-bi	τ_{max}	$\frac{3}{2}\tau_{max}$

Simulation results for conventional model and muscle model (mono-bi) in case of an external vertical force is shown in Figures 4.6 and Figure 4.7 As it is seen from graphs, for the same value of external forces, conventional model fails when the external force exceeds 43N; but model with monoarticular and biarticular muscle

mechanism does not fail for even 60N. The reason for such difference is that, because of the use of biarticular maximum possible joint torque can be increased by keeping the total torque of actuators.

The tracking error of conventional method is smaller than the tracking error of muscle model. One of the reasons for such difference is that, direct joint angle control is performed in conventional method; but in muscle model, the torques are shared by different muscles and the displacements of muscles are controlled. Because of using a spring-damper system to achieve muscle elasticity, the tracking error became higher; but on the other hand, the maximum external force that can be rejected became higher. Moreover, the torque output errors for each muscle are added to each other which results in more trajectory tracking error. The reason why there is a tracking error in the first 0.1s is because of the initialization problem of each muscle torques.

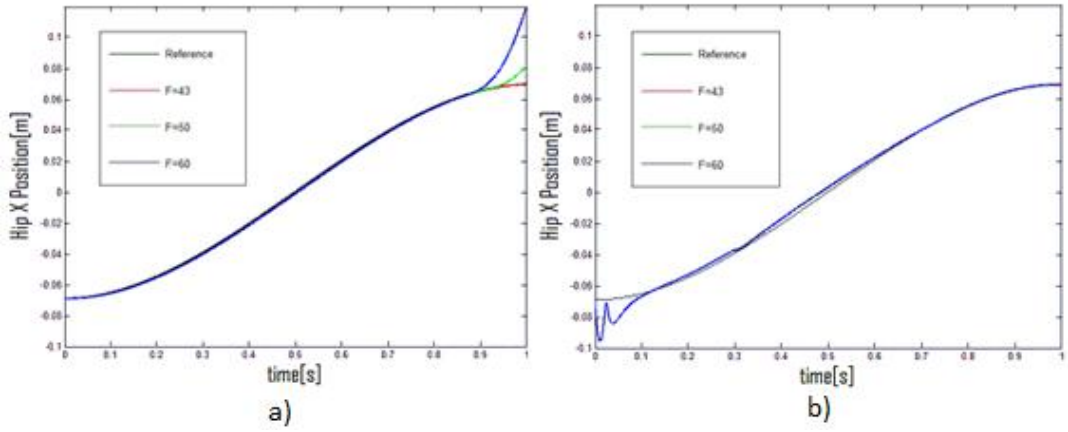

Figure 4.6 X Position outputs for different external forces for a)conventional model b)muscle model (F=43-50-60N)

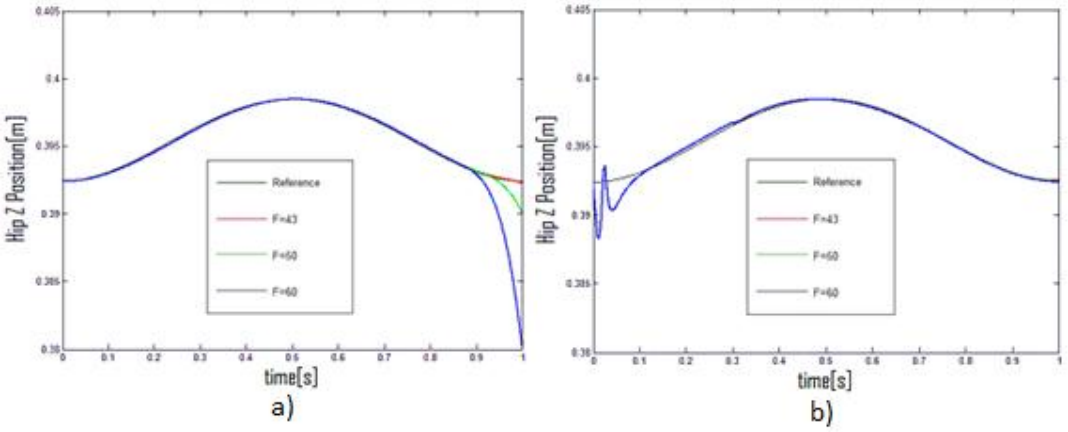

Figure 4.7 Z Position outputs for different external forces for a)conventional model b)muscle model (F=43-50-60N)

In order to show the maximum external force that robotic leg with muscle model can afford, one more simulation is done and the output of x and z positions and the posture of the leg is shown on Figures 4.8 and 4.9

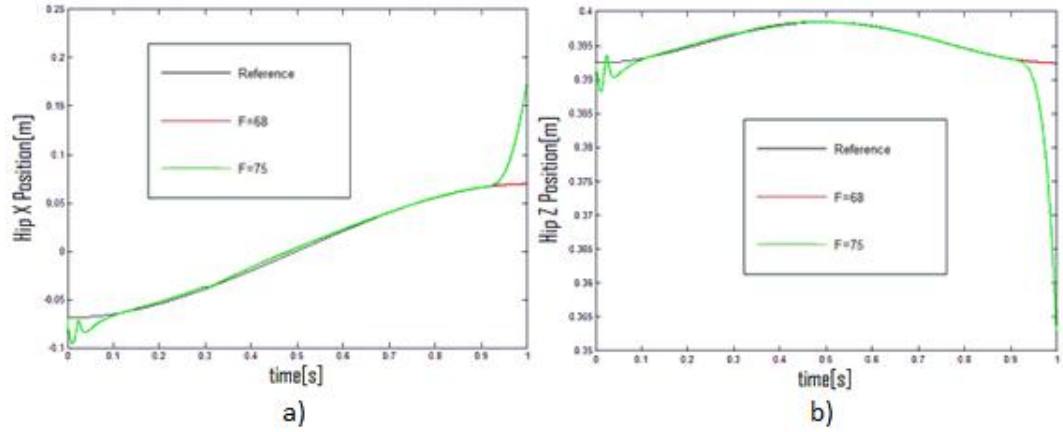

Figure 4.8 X and Z positions of hip in muscle model for F=68 and F=75

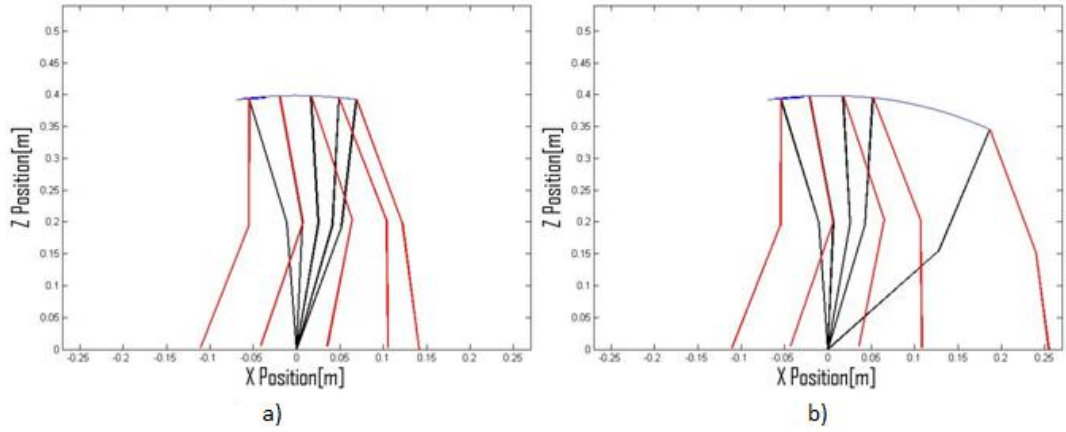

Figure 4.9 Posture of robotic leg with muscle model for a)F=68 b)F=75

Conventional model was able to reject an external force up to 43N; but muscle model is able to reject an external force up to 68N. The same simulations are also done for Case2 and resulting results are shown in Figures 4.10 and Figure 4.11

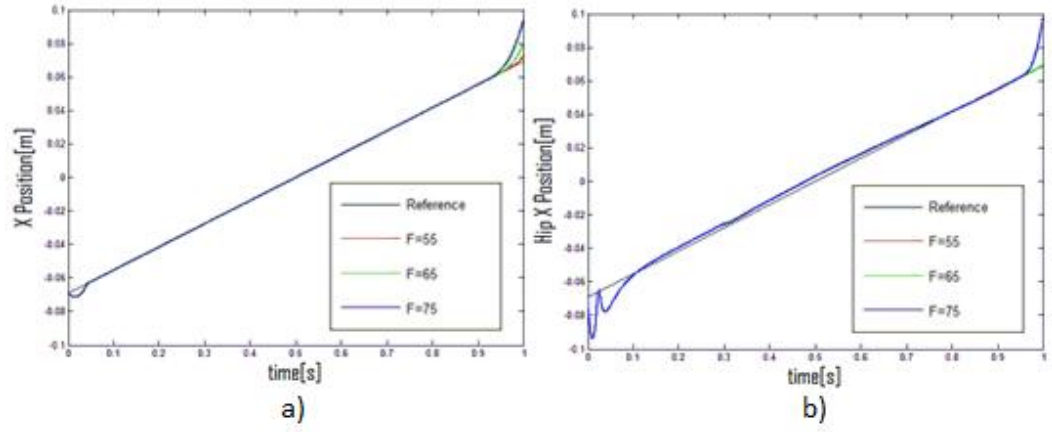

Figure 4.10 X Position outputs for different external forces for a)conventional model b)muscle model (F=55-65-75N)

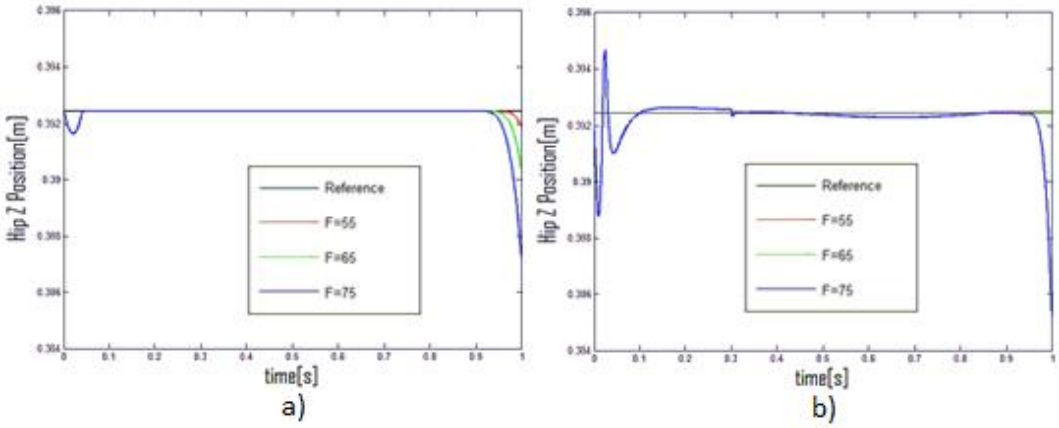

Figure 4.11 Z position outputs for different external forces for a)conventional model b)muscle model (F=55-65-75N)

It can be said from Figures 4.10 and 4.11 that, conventional model starts to fail for lower external vertical force in compared to muscle model. The deflections starts to occur above 55N for conventional model; but in muscle model even if the force is 65N, it looks like it does not start to deflect yet. But for 75N, none of methods are able to keep the robotic legs posture.

4.3.2 Comparison of Stability with and without Biarticular Muscle

In order to show the advantage of using biarticular muscle in self-stability of the robotic leg, two different simulations are done. In two cases, motion of robotic leg is performed by only two monoarticular muscle. In the first simulation, biarticular muscle is not present and an external force of 80N and 90N is acted on the robotic leg at t=0.3s. In the second simulation, biarticular muscle is present and the same external force is acted on the robotic leg at the same time. The resulting simulations show the difference between using biarticular muscle or not in tracking error and angular deflections of knee and ankle joints clearly. The deflections in x-direction is shown for two cases in Figure 4.12 and the deflections in z-direction is shown for two cases in Figure 4.13

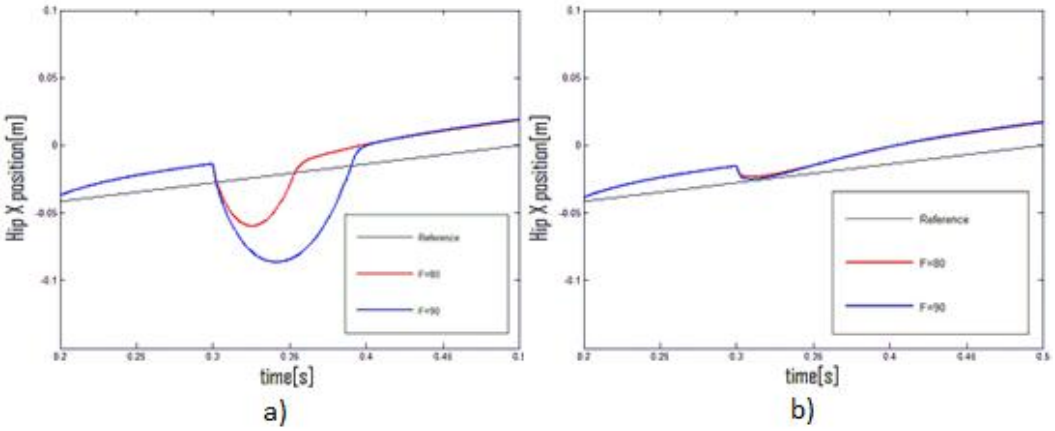

Figure 4.12 X position outputs for a) without biarticular b) with biarticular

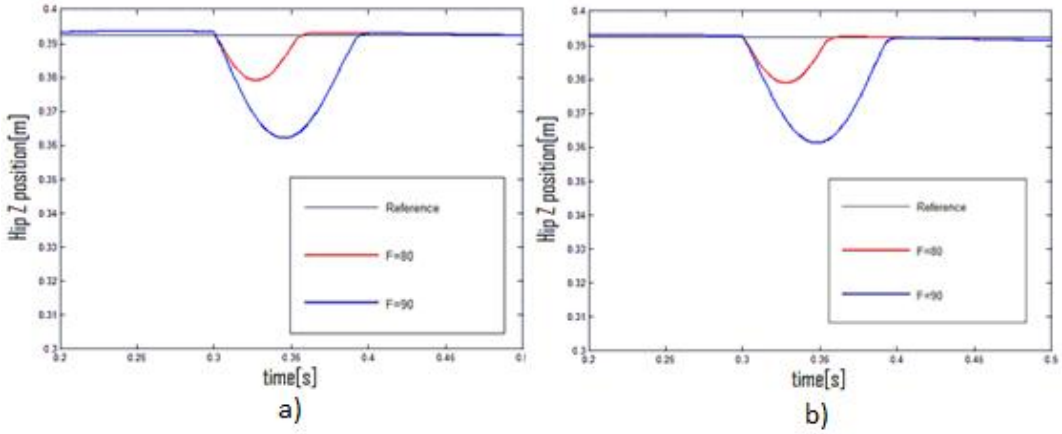

Figure 4.13 Z position outputs for a) without biarticular b) with biarticular

By looking at these figures, it can be said that biarticular muscle has improved the stability of the robotic leg especially in x-direction. In Figure 4.12.a, the deflection in x-direction is bigger than the deflection in x-direction in Figure 4.12.b. The reason behind this difference is that, biarticular muscle transfer energy between two adjacent joints. The deflection in one joint effects the other joint. When the knee angle deflects, the energy is transferred from knee joint to ankle joint, so that ankle joint will also deflect a little in order to keep the balance. Moreover, when the deflection occurs, biarticular muscle automatically exerts an opposing force at the edge of the joint so that the angular deflections also become lower. The deflection in vertical direction in Figure 4.13.a is close to the deflection in vertical direction is Figure 4.13.b; but trajectory tracking error becomes lower in case of using biarticular muscle.

Hip X and Z position is shown on Figure 4.14 for two schemes, without biarticular and with biarticular, in case of an external force of 80N. It can be clearly seen that the deflection is bigger in both directions. It is realized from this figure that, using biarticular muscle is effective for improvement in self-stability of robotic leg which is the most important fact to keep the balance in walking motion.

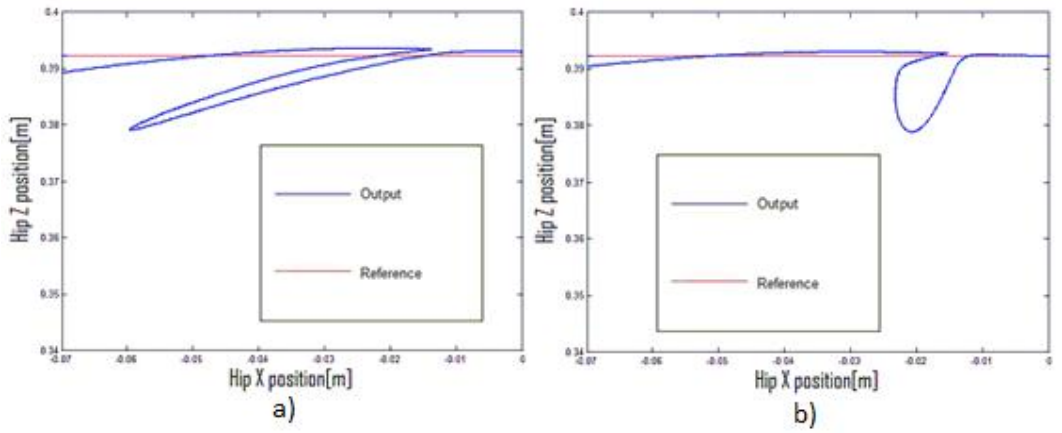

Figure 4.14 Hip positions a)without biarticular muscle b)with biarticular muscle

4.4 Discussions on Simulation Results

In this part, some comments and discussions about comparison between conventional and muscle model will be given.

4.4.1 Comments on Simulation Results

In the conventional model, the robotic leg is stiffer compared to the model that uses muscular system. When the force is started to be acted on hip of the robotic leg in vertical direction at t=0.3s, there is more deflection in the muscle model than the conventional model which was expected to happen because of the elasticity of muscles. The deflection increases as the external force increases; but in conventional model the deflection does not change much according to the magnitude of external force, but in case of a very high external force both models fail and the deflections would be high. The maximum torque that can be produced on joints has a limitation so that it is impossible to reject very high external torques.

Tracking error is more in muscle model than the conventional model. Since conventional model directly control the knee and ankle angles, position errors are smaller. In the muscle model, the joint torques are distributed among individual muscles and muscle displacements are taken as reference. The lengths of muscles and magnitudes of forces acting by muscles on the edge of joints are controlled. Because of the elasticity of muscles and distributed torque generation, there are more actuators to control in coordination with others. Torque errors of muscles which are connected to same joint are added to each other which causes the error to increase. In order to eliminate that error, more precise controllers may be designed for each muscle so that the total errors would also become smaller. But in the present trajectory tracking error, it does not seem fatal, because error is less than 2 mm. Trajectory tracking error in conventional model is lower; but the external force rejection capability is not better than muscle model. It is more essential to reject much force with small tracking error than rejecting low force with nearly no error since the stability of robotic leg is considered and the external force rejection capability is analyzed.

If a comparison between conventional model and muscle model in case of maximum external force rejection performances is done, the muscle model performs better, that is because of the fact that biarticular muscle transfer energy between two adjacent joint. As it was also discussed in Chapter 2.4, the maximum end point force magnitude and distribution is better in compared to conventional model. Conventional model was able to reject up to 43N for Case1 and 55N for Case2; but muscle mode was able to reject up to 68N for Case1 and 70N for Case2.

Moreover, in the case of using biarticular muscle the self-stability of the robotic leg is achieved better in comparison to not using biarticular muscle. The deflection in x-direction is smaller compared to not using biarticular muscle. The most interesting result that is obtained from the analysis on biarticular muscle in this research is its effect on self-stability.

4.4.2 Discussion on What is Better compared to Conventional Model

The advantages of muscle model against conventional model can be itemized as follows:

- Because of the elasticity of muscles, muscle model is more robust to sudden changes and hard to be broken; but conventional model is stiffer
- The distribution of end effector force is more homogenous and the maximum end effector force in the direction from ankle to hip is higher in muscle model which results in more external force rejection capability in vertical direction
- Even if the position control is problematic, muscles can exert opposite forces automatically as the deflection in joint angles increase
- Since biarticular muscles are connected to two adjacent joints and exert the same torque in these two joints; the total torque of actuators is smaller in compared to total torque actuators in conventional model
- Biarticular muscle is useful for robot to keep its balance, especially for horizontal direction; because biarticular muscles transfer energy between two adjacent joints. A deflection in one joint effects the other joint and robotic leg becomes more stable.

4.5 Summary of Chapter

Parameters that are used in the simulation are given. Then, simulation results for different external forces in conventional model and muscle model are shown in terms of position tracking performance and maximum external force rejection capabilities. Moreover, simulations are done in two different cases to show the efficiency of using biarticular muscles. In both cases, it is understood that using biarticular muscle makes robotic leg possible to reject more external forces in vertical direction in compared to conventional model. Furthermore, in the simulations, it is also realized that the deflection in x-direction can be compensated better in case of using biarticular muscle. Finally, discussion and comments about simulation results are given and the comparison between various methods are discussed.

Chapter 5

Conclusions and Future Works

5.1 Conclusions

5.1.1 Summary

In Chapter1, an introduction to humanoid robots with some examples are provided, the motivation and the general structure of this research is also presented.

In Chapter2, after giving a brief review of previous and on-going researches, the strategy to use monoarticular and biarticular muscles for simultaneous drive of two joints is proposed. Then, the difference between conventional robot control method and proposed method is clarified. Moreover, the distribution of the end effector force is explained in the case of using biarticular muscle, and compared with the conventional type.

In Chapter 3, theoretical and mathematical representations of robotic leg with muscle model are provided in detail. After giving the outline of the robotic leg motion, walking scheme, trajectory planning, calculations for angles, angular velocities, angular accelerations and joint torques are presented. The method to calculate individual muscle torques from joint torques is explained. Moreover, the effect of external forces on joint torques is given and the strategy to reject that force is explained. Resulted muscle displacement calculations are shown and the method to control each muscle torque is discussed. Finally, control diagram for muscles is provided.

In Chapter4, parameters that are used in the simulation are given. Then, simulation results for different external forces in conventional model and muscle model are shown in terms of position tracking performance and maximum external force rejection capabilities. Moreover, simulations are done in two different cases to show the efficiency of using biarticular muscles. Discussion and comments about simulation results are given and the comparison between various methods are discussed.

5.1.2 Conclusions

It was expected that in the muscle model, the total possible torque generated on joints would be higher which results to more external force rejection capability. As it can be seen from simulation results, total torque that is required on the joints is shared by mono and biarticular muscles and muscles are controlled successfully by a DC motor with a spring-damper system. The maximum external force that can be rejected by using musculoskeletal system is higher than the force rejected by using conventional model; but the tracking performance is a little worse than the performance in conventional model; since conventional model directly controls the joint angles. In the muscle model, the joint torques are distributed among individual muscles and muscle displacements are taken as reference. Torque errors of muscles which are connected to same joint are added to each other which causes the error to increase. In order to eliminate that error, more precise controllers may be designed for each muscle so that the total errors would also become smaller. But in the present trajectory tracking error, it does not seem fatal, because error is less than 2 mm.

The self-stability of robotic leg improves in case of using biarticular muscle. Biarticular muscle helps robotic leg to balance its posture, especially in x-direction by transferring energy between two joints. What is meant by energy transfer is that, when a deflection in knee angle occurs, there is change in the length of biarticular muscle which results in change in torque produced. That change in torque also effects ankle angle so that it also deflect. These deflections occur in a way that deflections in x-direction become smaller. Additionally, biarticular muscles exert an opposing force when an unexpected deflection in the angles occurs because of the spring system that is used in biarticular muscle.

Although it is difficult to achieve simultaneous control of such muscles, it can be relied on muscles' viscoelasticity in the very early response against external forces in control algorithms.

5.2 Future Works

Optimization of individual muscle torque calculation can be analyzed more and the tracking control can be improved. Further study should be done to improve the numerical analysis, such as including the effects of friction, efficiency of motor gear. In addition stiffness control can be implemented to achieve better external force rejection. In the existence of large external force, the stiffness can be increased for faster and more precise motion.

Verification of using monoarticular and biarticular muscles in robotic leg walking motion in case of a vertical external force by using feedforward strategy is done in simulation environment; but it is also required to build the real experimental system and observe the real reaction of whole system against external forces.

APPENDIX A

Proof of 2-Norm Approach

The problem can be written as;

$$\min \sqrt{\frac{x^2}{\max(x)^2}+\frac{y^2}{\max(y)^2}+\frac{z^2}{\max(z)^2}} \tag{A.1}$$

$$\begin{aligned}\tau_1 &= x+z\\ \tau_2 &= y+z\end{aligned} \tag{A.2}$$

where τ_1 and τ_2 are the joint torques, x, y, z denote the individual muscle torques and $\max(x), \max(y), \max(z)$ denote the maximum individual muscle torques.

The solution (x, y, z) should satisfy the following 3 criterias:

1. They should be on the line

$$\begin{aligned}\tau_1 &= x+z\\ \tau_2 &= y+z\end{aligned} \tag{A.2}$$

2. They should be on the surface of ellipse defined by

$$\frac{x^2}{\max(x)^2}+\frac{y^2}{\max(y)^2}+\frac{z^2}{\max(z)^2}=c \tag{A.3}$$

where c is a constant

3. The plane that pass through the lines defined by (A.2) should be tangent to the ellipsoid defined by (A.3), which gives the following equation

$$\frac{1}{\max(x)^2}\frac{\partial x^2}{\partial x}+\frac{1}{\max(y)^2}\frac{\partial y^2}{\partial y}+\frac{1}{\max(z)^2}\frac{\partial z^2}{\partial z}=0 \tag{A.4}$$

By combining all these 3 requirements, the solution becomes

$$x = \frac{(\tau_1 - \tau_2)\max(x)^2 \max(z)^2 + \tau_1 \max(x)^2 \max(y)^2}{\max(x)^2 \max(z)^2 + \max(x)^2 \max(y)^2 + \max(y)^2 \max(z)^2}$$
$$y = \frac{\tau_2 \max(x)^2 \max(y)^2 + (\tau_2 - \tau_1)\max(y)^2 \max(z)^2}{\max(x)^2 \max(z)^2 + \max(x)^2 \max(y)^2 + \max(y)^2 \max(z)^2} \quad \text{(A.5)}$$
$$z = \frac{\tau_1 \max(y)^2 \max(z)^2 + \tau_2 \max(x)^2 \max(z)^2}{\max(x)^2 \max(z)^2 + \max(x)^2 \max(y)^2 + \max(y)^2 \max(z)^2}$$

APPENDIX B

DC Motor Position Control Schematic

The detailed model that is used for muscle control is seen in Figure AppendixB.1 below.

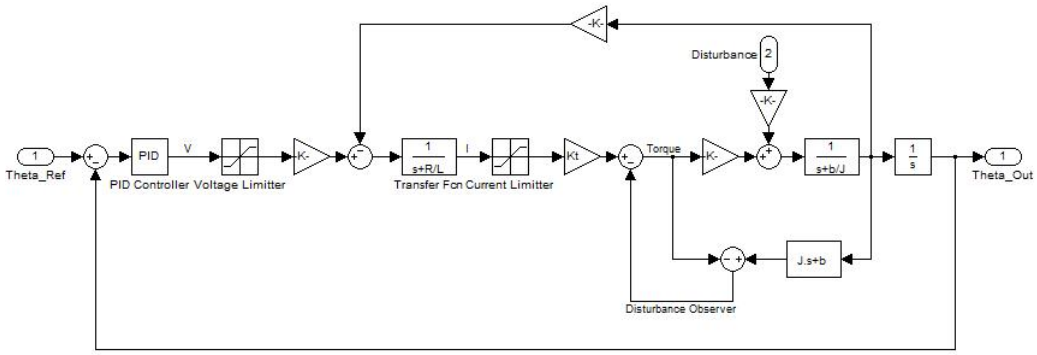

Figure AppendixB.1 Model of DC Motor Position Control under Disturbance

The desired position of DC motor is taken reference from muscle displacements. The equations for motor side and armature side is expressed as;

$$J\ddot{\theta} + b\dot{\theta} = K_t i(t) + \tau_{ex}$$
$$L\frac{di(t)}{dt} + Ri(t) = V - K_e\dot{\theta} \qquad \text{(B.1)}$$

where τ_{ex} is the external torque that opposes the rotation of DC motor and the magnitude is the resulted muscle torques.

Since the maximum voltage that can be applied to DC motor is limited to 24V and the current is 5A, voltage limiter and current limiters are used in order to keep the safety of DC motor.

To estimate the resulting torque errors, a disturbance observer is used. It basically takes the difference between generated torque and output torque as a feedback to the system so that there would not be much torque error outputs.

APPENDIX C

An external vertical force of 200N is applied on the hip position of both conventional model and muscle model. The resultant position of hip and the leg which is contact with the ground is shown in Figure AppendixC.1 and AppendixC.2 below

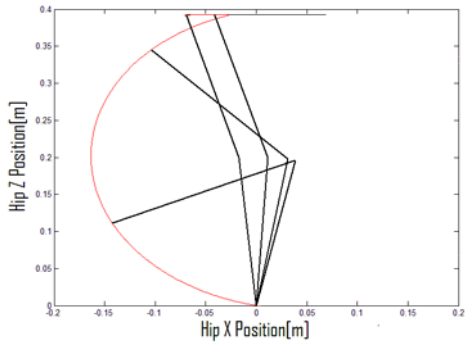

Figure AppendixC.1 Hip position for F=200N in conventional model

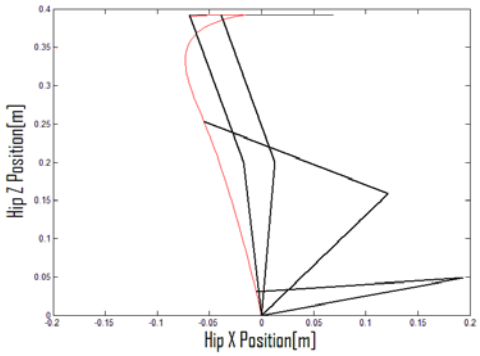

Figure AppendixC.1 Hip Position for F=200N in muscle model

By looking at these figures, for an excessive external force of 200N will result a fatal failure for both method; because it becomes impossible to exert necessary torque on joints due to the fact that actuators have limitation of maximum torques. Since there is a biarticular muscle present in muscle model, the robotic leg also tries to compensate the knee angle deflection by transferring energy between knee joint and ankle joint; but for that kind of a big external force, it is not sufficient to keep the posture.

Bibliography

[1] Endo K., Herr H., “Human Walking Model Predicts Joint Mechanics, Electromyography and Mechanical Economy”, October 11-15, 2009 St. Louis, USA, The 2009 IEEE/RSJ International Conference on Intelligent Robots and Systems

[2] Huang Y., et al, “Energetic efficiency and stability of dynamic bipedal walking gaits with different step lengths”, October 18-22, 2010, Taipei, Taiwan, The 2010 IEEE/RSJ International Conference on Intelligent Robots and Systems

[3]Zang Y. ,Yasuno T., Nogami R., Suzuki H., “Adaptive Walking Control Using CPG Network for Quadruped Robot with Bi-articular Muscles Model”, August 18-21,2010, The Grand Hotel, Taipei, Taiwan, SICE Annual Conference 2010

[4] Babic J., “Biarticular Legged Robot: Design and Experiments”, February 21 - 26, 2009, Bangkok, Thailand, Proceedings of the 2008 IEEE International Conference on Robotics and Biomimetics

[5] Iida F., Rummel J., Seyfarth A., “Bipedal walking and running with spring-like biarticular muscles”, 2008, Journal of Biomechanics 41 (2008), 656-667

[6]Fukusho H. , Koseki T., “Control of a Straight Line Motion for a Two-Link Robot Arm Using Coordinate Transform of Bi-articular Simultaneous Drive”, March 21-24, 2010, Nagaoka, Japan, The 11th IEEE International Workshop on Advanced Motion Control

[7] Babic J., Lim B., Omrcen D., Lenarcic J., Park F.C., “A Biarticulated Robotic Leg for Jumping Movements: Theory and Experiments”, February 2009, Vol 1/011013, Journal of Mechanisms and Robotics

[8] Rummel J., Blum Y., Maus H.M. Rode, C., Seyfarth, A., “Stable and Robust Walking with Compliant Legs”, May 3-8, 2010, Anchorage, Alaska, USA, 2010 IEEE International Conference on Robotics and Automation

[9] Endo K., Herr H., “A Model of Muscle-Tendon Function in Human Walking”, May 12-17, 2009, Kobe International Conference Center Kobe, Japan, 2009 IEEE International Conference on Robotics and Automation

[10] Yoshida K, Hata N., Oh S., Hori Y. “Extended Manipulability Measure and Application for Robot Arm Equipped with Bi-articular Driving Mechanism”, 2009

[11]BigDog - The Most Advanced Rough-Terrain Robot on Earth, Boston Dynamics, http://www.bostondynamics.com/robot_bigdog.html (visited on 30.01.2012)

[12]Niiyama R., Nagakubo A., Kuniyoshi Y., “Mowgli: A Bipedal Jumping and Landing Robot with an Artificial Musculoskeletal System”, April 10-14,2007, Rome, Italy, IEEE International Conference on Robotics and Automation, Page(s): 2546 – 2551

[13]Hosoda K., Takayama, H., Takuma, T., “Bouncing monopod with bio-mimetic muscular-skeleton system”, September 22-26, 2008, Nice, France, IEEE/RSJ International Conference on Intelligent Robots and Systems, Page(s): 3083–3088

[14] Watanabe, W., Sato, T., Ishiguro, A., *“An efficient decentralized learning by exploiting biarticular muscles - A case study with a 2D serpentine robot”*, May 19-23 2008, Pasadena, CA, USA, IEEE International Conference on Robotics and Automation, Page(s): 3826 - 3831

Publications

Technical Meetings

[1]Duman E., Koseki T., *"Walking Control of Multiple Link Robotic Leg under External Forces by Emulating Functionality of Combined Mono and Bi-Articular Muscles",* December 20, 2011, Tokyo, JAPAN, Control Technical Meeting, The Institute of Electrical Engineers of Japan